

Study of Collisional Plasma Sheath using Kinetic Trajectory Simulation (KTS)

A Dissertation

Submitted to the Central Department of Physics

University Campus, Tribhuvan University

Kirtipur, Kathmandu, Nepal

in the Partial Fulfillment for the Requirement of

Master's Degree of Science in Physics

By

Bhim Bahadur Bam

February, 2014

Contents

Recommendation	i
Acknowledgements	ii
Evaluation	iii
Abstract	iv
1 Introduction	1
1.1 Plasma	2
1.2 Sheath	5
1.3 Presheath	6
1.4 Collision in plasma	7
1.5 Collision in sheath	8
1.6 Scope and applications	8
2 Review of Plasma Sheath	10
3 Principle of Kinetic Trajectory Simulation (KTS)	15
3.1 About KTS model	16
3.2 Basic concepts of kinetic theory	16
3.2.1 For collisionless case	18
3.2.2 For collisional case	18
3.3 Basic equations	19

3.4	Boundary conditions	21
4	The Plasma Sheath Model	22
4.1	Description of the model	23
4.2	Boundary conditions	24
4.3	Bohm criterion	30
4.4	Presheath-sheath approximation	32
4.4.1	Presheath	33
4.4.2	Sheath	34
4.4.3	Presheath-Sheath coupling	34
5	Numerical Method	36
5.1	Discretization of the simulation region	37
5.2	Electron density distribution	39
5.3	Discretizing ion velocity space with a fixed grid	40
5.4	Ion trajectories	40
5.4.1	Discrete set of the injection velocities	40
5.4.2	Discrete set of ion trajectories	40
5.4.3	Numerical calculation of ion trajectories	41
5.4.4	Intersection velocities	42
5.5	Ion velocity distribution function	44
5.6	Ion density distribution	44
5.7	Solution of Poisson's equation	45
5.8	Relaxation scheme	46
5.9	Electric field calculation	47
5.10	Iteration scheme	49
5.11	Main iteration block	50
5.12	Convergence check	52
5.13	Numerical parameters	52

<i>CONTENTS</i>	3
6 Results and Discussion	53
6.1 Ion density profile	54
6.2 Electron density profile	55
6.3 Comparison between ion and electron density profile	57
6.4 Potential profile	58
6.5 Electric field profile	59
6.6 Total charge density profile	60
6.7 Average ion velocity profile	61
6.8 Ion effective temperature profile	62
6.9 Discussion and conclusion	63
Appendix	65
A Matlab Files	65
Bibliography	81

RECOMMENDATION

It is certified that **Mr. Bhim Bahadur Bam** has carried out the dissertation work entitled
“Study of the Collisional Plasma Sheath using Kinetic Trajectory Simulation ”.

I recommend the dissertation in the partial fulfillment for the requirement of Master's Degree of Science in Physics at Tribhuvan University.

.....
Dr. Raju Khanal
Central Department of Physics
Tribhuvan University, Kirtipur
Kathmandu, Nepal

Date:

ACKNOWLEDGEMENTS

It is my unspeakable bliss to put forward my few words to express cordial, respectful gratitude to my supervisor cum guide, **Dr. Raju khanal** of the Central Department of Physics, T.U., Kirtipur for guiding me so well that I never felt the task - a burden, instead I feel now a part of enjoyment is getting over. He also deserves thankfulness for treating me as his equal as a human being and as a learner simultaneously. I would be mean, stingy if I could forget his lively smile, co-operative friendliness and his internal drive for inspiring others. Moreover, I dare not coin any words for his superb hospitality. This happening was an exotic, soothing and heavenly coincidence, I have felt and cherished.

I would like to express my gratitude to all the members of the Central Department of Physics for their direct or indirect contribution in carrying out this research work. Similarly, my thanks also go to all my colleagues for their help and encouragement. I should not forget to extend my thankfulness to all the informants for their kind co-operation and response and also for their encouragement, suggestions and request to carry out further research on different aspects of collisional sheath.

At last but not the least, I would like thanks to all my family members for their supports and encouragement throughout my life. Without their support, it is impossible for me to complete my Master's Degree.

EVALUATION

We certify that we have evaluated this dissertation entitled "**Study of the Collisional Plasma Sheath using KTS**" submitted by **Mr. Bhim Bahadur Bam** and in our opinion, it fulfills all the specified criteria, in the scope and quality, as a dissertation for the partial fulfillment of the requirement for the degree of Master of Science in Physics at Tribhuvan University, Kirtipur, Kathmandu, Nepal.

Evaluation Committee

Dr. Raju Khanal

(Supervisor)

Dr. Binil Aryal (Head)

Central Department of Physics
Tribhuvan University, Kirtipur

Kathmandu, Nepal

External Examiner

Internal Examiner

Date:.....

ABSTRACT

In all practical application of plasma, the sheath formed close to wall material plays an crucial role in determining the property of over all plasma wall transition. Mostly collisionless sheath were studied using fluid model and kinetic model but it is the first time we try to study collisional sheath using Kinetic Trajectory Simulation model by introducing general collision term explicit dependence on a constant α , which determines the degree of collision. In this model, the distribution function of the particles species are directly calculated by solving the related collisionless and time-independent kinetic equation along the respective particles trajectories. We vary the value of alpha from 0 which is for collisionless case to 1 and study the different sheath parameters. But increasing α after certain value there is no significant change in sheath parameters due to saturation in sheath. The result obtained is expected to be useful in controlling flow of plasma particles at the wall. Our study has crucial importance in material processing, plasma etching and for confinement of plasma in fusion devices.

Chapter 1

Introduction

1.1 Plasma

The term plasma was introduced by Langmuir in 1928 to describe the state of matter in the positive column of glow discharge tubes [1]. The word plasma means something molded or fabricated (comes from Greek word $\Pi\lambda\alpha\sigma\mu\alpha$). The existence of plasma as the fourth state of matter was first identified by Sir W. Crooks in 1879 (he called it radiant matter) [2]. If temperature of gas increased beyond a certain limit , it does not remain a gas, it enter a region where the thermal energy of it's constituent particle is so great that the electrostatic forces which binds electron to atomic nuclei are overcome. Instead of hot gas composed of electrically neutral atoms, we have mixed population of charged and neutral particles. This is a plasma, and it is neither solid, liquid nor gas. But any ionized gas can not be plasma [3], there is always some small degree of ionization in any gas given by Shahas Equation. The amount of ionization to be expected in a gas in thermal equilibrium is given by Saha equation:

$$\frac{n^i}{n^n} \approx 2.4 \times 10^{21} \frac{T^{3/2}}{n^i} e^{-U_i/k_B T} \quad (1.1)$$

where n^i and n^n are respectively, the number density of ionized atoms and neutral atoms, T is the gas temperature in Kelvin, k_B is Boltzmann's constant, U_i is the ionization energy of the gas. For ordinary gas at room temperature, we can take $n^n \approx 3 \times 10^{25} \text{ m}^{-3}$, $T \approx 300^\circ \text{ K}$, and $U_i = 14.5 \text{ eV}$ (for Nitrogen). The fractional ionization is low:

$$\frac{n^i}{n^n} \approx 10^{-122} \quad (1.2)$$

As the temperature is raised, the degree of ionization remains low until U_i is only a few times $k_B T$. Then n^i/n^n rise abruptly, and the gas is in a plasma state. Further increase in temperature makes n^n less than n^i , and the plasma eventually becomes fully ionized.

Thus plasma is quasineutral gas that shows collective behavior. Quasineutrality means electron density and ion density are nearly equal ($n_i \approx n_e \approx n$, where n is density of plasma) but not so neutral that all the interesting electromagnetic vanish. Collective behavior of

plasma implies that the dynamics of plasma particles depends not only on the local condition but also on the state of plasma far away from the point of interest [3].

Any ionized gas can be called plasma if it fulfill the flowing criterion

- 1) $\lambda_D \ll L$ (Debye shielding).
- 2) The number of particle in Debye sphere is very large, $N_D \gg 1$.
- 3) $\omega_p \tau > 1$, where ω_p is plasma frequency and τ is mean time between the collision with neutral atoms.

A fundamental property of plasma is its ability to shield out any external electric potential applied to it. Before external applied potential to plasma, the plasma potential $\phi \cong 0$ every where because ion and electron densities (-ve and +ve charge density) were spatially uniform and equal. The particle having same polarity as the test charge (used to apply external potential) will be repelled where as particle of opposite polarity will be attracted. In the way the test charge surrounded by the opposite charge to that of test charge to alleviate it's effect on remaining bulk of plasma. i.e external potential shielded in a small. This phenomenon is called Debye shielding. This region is generally considered as spherical in shape being test particle at centre, known as Debye sphere and radius of this sphere is called Debye length. As shown in figure 1.1.

The typical expression for the electron Debye length with electron temperature T^e and common density n^e is given by

$$\lambda_D^e = \sqrt{\frac{\epsilon_0 k_B T^e}{e^2 n^e}}. \quad (1.3)$$

The picture of Debye shielding [cf. Fig. 1.1] that we have given is valid only if there are enough particles in the charge cloud. Clearly, if there are only one or two particles in the sheath region, Debye shielding would not be a statistically valid concept.

$$N_D = \frac{4}{3} \pi \lambda_D^3 \quad (1.4)$$

As ion are massive than electron can be considered as uniform back ground in plasma (

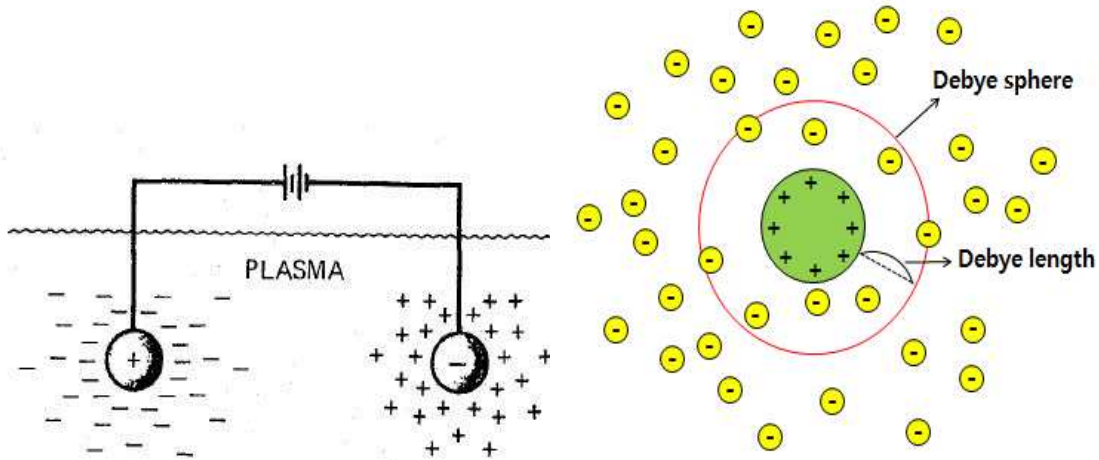


Figure 1.1: Debye shielding.

plasma approximation). If the electron in plasma are displaced uniform back ground of ion, a electric field will be built up in such a way as to restore the neutrality of the plasma by pulling the electron back to their equilibrium position. Because of their inertia, the electron will be overshoot and oscillate around equilibrium position with a characteristic frequency known as plasma frequency. The expression for plasma frequency is given by

$$\omega_p = \sqrt{\frac{n_o e^2}{\epsilon_o m_e}} \quad (1.5)$$

Where n_o is plasma density, e and m_e respectively charge and mass of electron.

The third condition imply motion of plasma particles is controlled by electromagnetic forces rather than by ordinary hydrodynamic forces.

The study of plasma is crucial due to its application in various field like astro physics, material processing, surface treatment, fusion energy, semiconductor device etc. One of vital source of energy is sun in which nuclear fusion reaction takes place and the energy produces continuously same as in stars [5]. Various methods for the terrestrial realization of fusion energy have been explored so far but confinement of plasma is one the challenging problem in fusion. In such fusion devices where the plasma comes into contact with a wall, the plasma region near the wall plays an important role in determining the overall plasma properties

which is known as the “sheath”.

1.2 Sheath

In the production of plasma energy supplied to gas in order ionize is not problem but problem is that how to confine it for a certain time. For any practical use it must has to come in contact with the material. When plasma comes in contact with suitable material due to high mobility of electron (due to lighter mass than ion) they hits the wall charging the material surface negative respect to bulk of plasma. As the negative potential of wall increases ions are attracted and it repels the part of electron. An equilibrium is finally reached when the potential difference is few times the electron temperature forming a positive space charge region is in between wall and bulk plasma known as sheath. Simply it can be stated that the sheath region is formed due to Debye shielding so scale of sheath will be few Debye length λ_D . The function of a sheath is to shield quasineutral plasma from the potential distortion caused by an absorbing negative wall. Due to the shielding effect of plasma, the negative potential at wall have stronf effect only in the sheath region which extended only to few Debye length away from the wall. Within this region the plasma is significantly non-neutral how ever becoming quasineutral at the sheath edge (also called “sheath entrance (SE)”). As we move very close the wall, the potential falls off rapidly. Due to decrease in the potential the electric field is strong and the motion of the particles is dominated by electric force rather than magnetic force. The sheath structure is responsible for the flow of the particles and the energy towards the wall and may also affect the bulk-plasma behavior [6, 7]. The sheath is dominated by large gradient of the electric field compared to that of presheath region. The Fig. 1.2 shows the schematic potential variation in front of a negative wall.

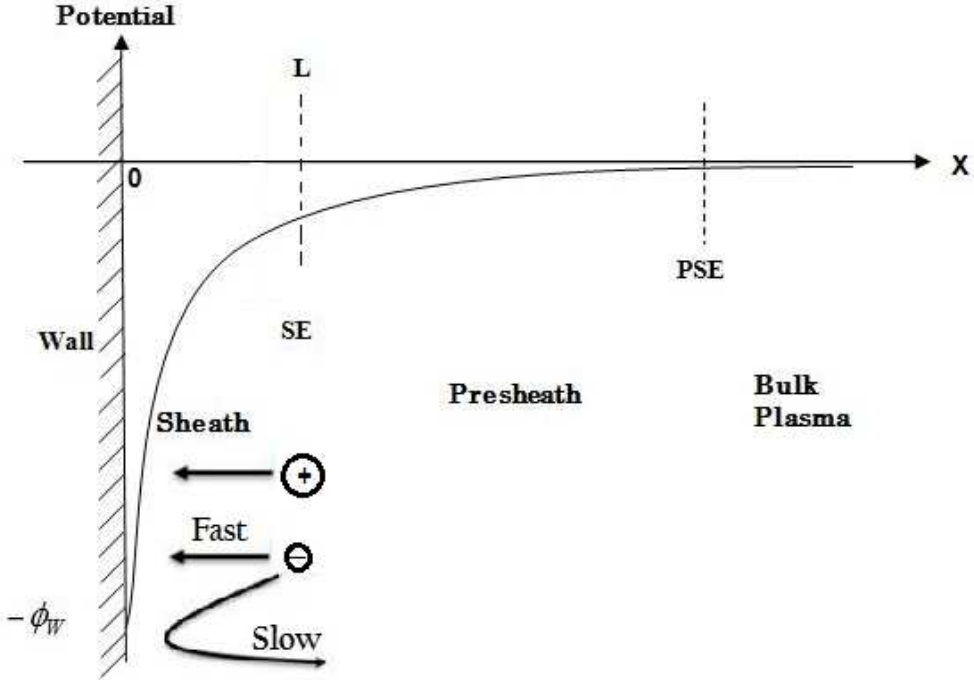


Figure 1.2: Schematic potential variation in front of a negative wall.

1.3 Presheath

A quasineutral region in between sheath and bulk plasma having length scale greater than sheath and less than bulk plasma formed [cf. Fig. 1.1] due to presence of weak electric field, which is due to not perfect shielding of wall potential, responsible for accelerating the ion to a velocity that satisfy Bohm criterion. The Bohm criteria [8] is

$$\langle \frac{1}{v^2} \rangle \leq \frac{1}{C_s^2} \quad (1.6)$$

where $\langle \rangle$ denotes averaging over the ion distribution function and

$$C_s = \sqrt{\frac{k_B(\gamma^i T_{ps}^i + \gamma^e T_{ps}^e)}{m^i}} \quad (1.7)$$

is the ion-acoustic velocity defined at the presheath side of the sheath edge. Here γ^i and γ^e are the ion and electron polytropic constants respectively and T_{ps}^i and T_{ps}^e are the ion and electron temperatures at the presheath side of the sheath edge respectively [6, 7].

Thus to form sheath ion must enters the sheath region with minimum or greater than ion acoustic velocity (C_s).

1.4 Collision in plasma

Study of collision process between micro particles of a system like fluid and plasma has great importance because such systems are usually associated with the collisions. By studying the collision, we can investigate the nature of the force existing between them. Not only investigate the nature of force, we can study different phenomenon in plasma. The collisions are also responsible for bringing the system about the ultimate Equilibrium situation where the Maxwellian distribution is prominent. The collisions between the particles may be elastic or inelastic. Elastic collisions, also called soft collisions or grazing collisions are collision in which there is no change in the internal energy of the colliding particles, these collisions are studied classically. In inelastic collision there is change in the internal energy of the colliding particles and they are studied quantum mechanically. It is noted that whether collision is elastic or inelastic there is always transfer of momentum between them. In the collision of neutral particles momentum transfer occurs only impulsively whereas in the collision of charged particles momentum is transferred continuously through grazing collisions. In the classical theory of collision, particles are taken as rigid and spherically symmetric point masses, having no spin and so having only three degrees of freedom due to only translational motion. The average of distances travelled between successive collisions is called the mean free path. Mean free path is taken as the average of distances travelled during a sequence of small angle collisions. The average time that is spent by a particle between two successive collisions is called the collision time.

In weakly ionized plasma collision between charged particles and neutral particles and between neutral particles and short range interaction. But the charged particles themselves interact mutually with a long range coulomb interaction. So, in weakly ionized plasma,

we consider both short and long range infraction. In fully ionized plasma, particles mutually infract with long range Coulomb force. Due to such long range infraction particles undergoes continuous deflection during their motion [9].

1.5 Collision in sheath

The collision in sheath not similar to collision in plasma because sheath is non-neutral due to high density of ions than electrons, sheath itself alone can not be called plasma. The collision in sheath region result of high density of ions, thus it is close to sufficient to account collision between ions.

1.6 Scope and applications

The collisional effect in sheath region have studied with help of Kinetic Trajectory Simulation (KTS) [16] with slight changes to include collision; as this model is expected to give more accurate result. In all practical application of plasma, it must come in contact with material where a sheath layer formed between material wall and bulk plasma. So it is crucial to have knowledge of sheath, different sheath parameter and different sheath phenomenon to work in field of plasma.

The plasma physics applied in various field like in nuclear physics, astro physics, surface treatment of material, plasma diagnosis etc.

The dissertation work is organized as introduction is given in chapter 1, in chapter 2, reviews of some related work are discussed. In chapter 3, the principle of KTS is discussed. In chapter 4, we describe the $1d1v$ plasma sheath model with boundary conditions, discuss the kinetic Bohm-Chodura criterion and the coupling of presheath and sheath. In chapter 5, we

discuss the numerical methods for the plasma sheath simulation where we have also described how our solution is iterated, starting from given boundary conditions to reach the final self-consistent state. In chapter 6, we have presented the results obtained with discussion and conclusion and numerical program (MATLAB) files are listed in the Appendix.

Chapter 2

Review of Plasma Sheath

Studies on confinement of plasma have always been a priority of interest for all practical plasma devices, specially for the magnetic confinement fusion device, where the plasma is confined in a vacuum chamber of a finite size. The study of plasma at the wall of the chamber has not yet been fully understood. However, several theoretical and practical works have been done. Some of which are reviewed below.

T . E. Sheridan and J. Goree investigated collisional sheath model [10], the effects of ion collisionality on the plasma sheath are revealed by a two-fluid model. The ion-neutral collision cross section is modeled using a power law dependence on ion energy. Exact numerical solutions of the model are used to determine the collisional dependence of the sheath width and the ion impact energy at the wall. Approximate analytical solutions appropriate for the collisionless and collisionally dominated regimes are derived. These approximate solutions are used to find the amount of collisionality at the center of the transition regime separating the collisionless and collisional regimes. Rx- the constant ion mean-free-path case, the center of the transition regime for the sheath width is at a sheath width of five mean-free paths. The center of the transition regime for the ion impact energy is at a sheath width of about one-half of a mean-free path.

S.Farhad Masoudi, Shadi S. Esmaeili, Shima Jazavandi study the ion dynamics in plasma sheath under the effect of $E \times B$ and collision force using fluid model. They investigated the velocity [11], kinetic energy and density distribution of ion in collisional and collisionless magnetic plasma sheath. Considering an external magnetic field, the ion moment under the effect of magnetic, electric and collisional force has been analyzed. It is shown that sheath thickness decreases by increasing the magnetic field strength and effect of collision on ion characteristics illustrated.

I. Langmuir was the first study of plasma by the basic features of the plasma sheath transition [7]. He studied the interaction of electron and positive ion space charges in sheaths. He

found that the potential distribution in the plasma, determines the motion of the ions and thus fixes the rate at which the ions arrive at sheath. In his investigations, the essence of Bohm criterion was used in an implicit form. In 1949, Bohm formulated and interpreted the sheath formation condition explicitly [8, 19].

H.-B. Valentini study that in collisional in slightly ionized plasmas, i.e. for many typical low pressure discharges, at the sheath edge the drift velocity of the plasma can be smaller than the ambipolar sound speed of the ions. This basic result demonstrated using simple analytical expressions. Under these conditions the Bohm criterion, in its usual formulation, is a sufficient condition for the existence of a positive boundary sheath, but it is not a necessary condition [13].

K. U. Riemann, F. Hermann and H. B. Valentini attempted to generalize the Bohm criterion for collisional case [?, ?, ?]. These attempts were based on an arbitrary definition of presheath and sheath regions. Riemann established a well-known and widely used subdivision of the boundary layer of a collision dominated plasma into a collisionless sheath and quasineutral presheath. This subdivision is strictly valid only in the case when $\frac{\lambda_D}{\lambda} \rightarrow 0$, where λ_D is the electron Debye length and λ is the ion mean free path [5]. The sheath edge separating the presheath and sheath is defined by the Bohm criterion. Riemann has used a simple fluid model of ions to account for collisions and space charges in boundary layer to clear the controversial statements on the validity of plasma sheath concept and on the role of Bohm criterion for finite value of $\frac{\lambda_D}{\lambda}$.

M. Goswami and H. Ramachandran illustrated a 1-D self consistent plasma column that includes both the sheath and the presheath [14]. They derived an analytic solution for interesting limit where the collision operator is independent of flow of velocities. They claimed that the most conspicuous feature of the boundary potential profile is the plasma sheath that is normally formed at plasma boundary to balance electron and ion flux loss. Electric

fields at sheath are normally much stronger than bulk plasma electric fields. In collisionless and weakly collisional systems, sheath scale lengths depend on Debye length, λ_D , and are normally much smaller than the plasma dimension, L .

Rui Rosa demonstrated a simple model of a collisional plasma sheath, with ionizing collisions included and in contact with a negative metal wall. A broad range of plasma sheath solutions is obtained and their properties are discussed. The characteristic of the abnormal glow discharge as well as the characteristic of the electrostatic probe, in the ionsaturation region, are incidentally recovered. This then applied to the study of current multiplication in electrical discharges. The properties of a plasma current multiplier are predicted, both in the low and high pressure regimes [15].

R. Khanal contributed in the development and understanding of the sheath by developing a kinetic model to study the space charge sheath adjacent to an absorbing wall. He coupled the kinetic sheath solution to a two-fluid presheath one. He described extensively the Kinetic Trajectory Simulation (KTS) model and how to obtain the final self consistent time-independent state. He devised and demonstrated this model only for *1d1v*, time-independent and collisionless cases and applied this model to the special case of a *1d1v* single emitter plasma diode for the purpose of testing and comparison. He used the KTS model to study a space charge sheath adjacent to an absorbing wall and bordering on a presheath described in a two-fluid model. The solution of related presheath-sheath coupling problem is developed, evaluated and discussed in detail. A comparison of the sheath model developed by him and the ‘standard’ one (having Boltzmann distribution electrons) shows qualitative agreement but also some discrepancies due to the different electron distributions [16].

V. Godyak suggested that the most prominent feature of the boundary potential profile is the plasma sheath that is normally formed at the plasma boundary to balance electron and ion flux [18]. According to him, Sheath electric field are much stronger than the bulk

plasma electric field and in collisionless and weakly collisional systems, sheath scale lengths depends on Debye length and are normally much smaller than the dimensional of plasma.

R. N Franklin study the conventional equations describing plasma and sheath are examined over a full range of collisionality to determine the influence of collisionality on the ion equation of motion that is, when the ion motion is essentially inertial and when it is collisional. When it is inertial in the sheath the Bohm criterion has been satisfied, while when the sheath is collisional the ions remain in equilibrium with the field all the way to the wall [17].

S. Farhad Masoudi investigated collisional sheath using external magnetic field [12], by considering collision between ions and neutral gas atoms under various pressure. He showed that ion density increase as collision effect than collision less case. Also in sheath near to wall the effect of magnetic field dominated by collision.

Chapter 3

Principle of Kinetic Trajectory

Simulation (KTS)

3.1 About KTS model

In the Kinetic Trajectory Simulation (KTS) the velocity distribution function of particle species involved are directly calculated by solving the related kinetic equations along the respective collisionless particle trajectory. In order to obtain the distribution function at any point of the phase-space we trace the related trajectories of phase-space where the distribution function is given. Here we assume the electron and ion velocity distribution function at the sheath edge to be cut-off Maxwellian.

KTS is an iterative method for numerically calculating self consistent, time-independent kinetic plasma states in some given bounded spatial region. The plasma states are generally characterized by,

- the velocity distribution function, $f(\mathbf{x}, \mathbf{v})$,
- the electric field, $\mathbf{E}(\mathbf{x})$,
- the magnetic field, $\mathbf{B}(\mathbf{x})$,
- collision term, $\mathbf{C}(\mathbf{x})$
- given boundary conditions.

3.2 Basic concepts of kinetic theory

At any given time, each particle has a specific position and velocity. We can therefore characterize the instantaneous configuration of a large number of particles by specifying the density of particles at each point \mathbf{r}, \mathbf{v} in phase-space. The function prescribing the instantaneous density of particles in phase-space is called the distribution function and is denoted by $f(\mathbf{r}, \mathbf{v}, t)$. Thus, $f(\mathbf{r}, \mathbf{v}, t)d\mathbf{r}d\mathbf{v}$ is the number of particles at time t having positions in the range between \mathbf{r} and $\mathbf{r}+d\mathbf{r}$ and velocities in the range between \mathbf{v} and $\mathbf{v} + d\mathbf{v}$. As time progresses, the particle motion and acceleration causes the number of particles in these \mathbf{r} and \mathbf{v} ranges to

change and so f will change. This temporal evolution of f gives a description of the system more detailed than a fluid description, but less detailed than following the trajectory of each individual particle. Using the evolution of f to characterize the system does not keep track of the trajectories of individual particles, but rather characterizes classes of particles having the same \mathbf{r}, \mathbf{v} [6]. In the general case of time-dependent, collisional kinetic theory, the species- s

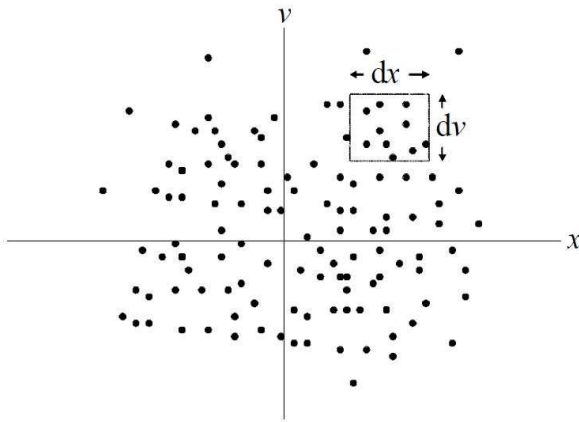


Figure 3.1: A box with in phase space having width dx and height dv in $1d1v$.

velocity distribution function satisfies the kinetic equation

$$\frac{d_s f^s}{dt} = \left(\frac{\partial}{\partial t} + \mathbf{v} \cdot \frac{\partial}{\partial \mathbf{r}} + \mathbf{a}^s \cdot \frac{\partial}{\partial \mathbf{v}^s} \right) f^s \quad (3.1)$$

$$= C^s, \quad (3.2)$$

with

$$\mathbf{a}^s(\mathbf{r}, \mathbf{v}, t) = \frac{q^s}{m^s} [\mathbf{E}(\mathbf{r}, t) + \mathbf{v} \times \mathbf{B}(\mathbf{r}, t)]. \quad (3.3)$$

Here, the macroscopic (i.e. space locally averaged) electric and magnetic fields are $\mathbf{E}(\mathbf{r}, t)$ and $\mathbf{B}(\mathbf{r}, t)$, the macroscopic acceleration of the species- s particles (i.e. its acceleration in these fields) is $\mathbf{a}^s(\mathbf{r}, \mathbf{v}, t)$, and C^s is the species-‘ s ’ collision term. The time derivative

$$\frac{d}{dt} \equiv \left(\frac{\partial}{\partial t} + \mathbf{v} \cdot \frac{\partial}{\partial \mathbf{r}} + \mathbf{a}^s \cdot \frac{\partial}{\partial \mathbf{v}} \right) \quad (3.4)$$

is the “Lagrangian” or total time derivative along the species ‘ s ’ trajectory.

3.2.1 For collisionless case

For collisionless cases the kinetic equation Eq. (4.2) takes the well known form of “Vlasov equation”

$$\left(\frac{\partial}{\partial t} + \mathbf{v} \cdot \frac{\partial}{\partial \mathbf{r}} + \mathbf{a}^s \cdot \frac{\partial}{\partial \mathbf{v}} \right) f^s = 0 \quad (3.5)$$

i.e.,

$$\begin{aligned} \frac{d}{dt} f^s &= 0 \\ f^s &= f_{st}^s = \text{constant.} \end{aligned} \quad (3.6)$$

where f_{st}^s is startiting distribution for species- s .

This means that the velocity distribution function is same as starting or constant for an observer moving along a collisionless trajectory. Hence, the distribution function at every point along the trajectory can be obtained if its value at one point is known. Here we assume the boundary distribution function is given.

3.2.2 For collisional case

For collisional case the kinetic Eq. (4.2) takes the form

$$\left(\frac{\partial}{\partial t} + \mathbf{v} \cdot \frac{\partial}{\partial \mathbf{r}} + \mathbf{a}^s \cdot \frac{\partial}{\partial \mathbf{v}} \right) f^s = C^s \quad (3.7)$$

i.e.,

$$\begin{aligned} \frac{d}{dt} f^s &= C^s \\ f^s &= f_{st}^s + I^s \end{aligned} \quad (3.8)$$

where f_{st}^s is startiting distribution for species- s and I^s is collision integral given by

$$I^s = \int C^s dt \quad (3.9)$$

This means that the velocity distribution function is not constant but changes for an observer moving along a collisionless trajectory. Hence, the distribution function at every point along

the trajectory can be obtained only if its value at one point and the effect of collision is known. Here we assume the boundary distribution function and collision term C^s is given.

3.3 Basic equations

The following basic equations correspond to one-dimensional, time-independent, collisional, electrostatic problems:

(a) For electrons ($q = -e$), $C^e = 0$ the velocity distribution function satisfies the time-independent Vlasov equation in differential form as

$$\frac{df^e}{dt} = \left[\mathbf{v} \cdot \frac{\partial}{\partial \mathbf{r}} - \frac{e}{m^e} (\mathbf{E}(\mathbf{r}) + \mathbf{v} \times \mathbf{B}(\mathbf{r})) \cdot \frac{\partial}{\partial \mathbf{v}} \right] f^e(\mathbf{r}, \mathbf{v}) \quad (3.10)$$

$$= C^e \quad (3.11)$$

and in trajectory integrated forms as:

$$f^e(\mathbf{r}, \mathbf{v}) = f_{st}^e(\mathbf{r}_{st}^e, \mathbf{v}_{st}^e), \quad (3.12)$$

where f_{st}^e is the “starting distribution”, \mathbf{r}_{st}^e is the starting configuration and \mathbf{v}_{st}^e is the starting velocity of electrons. The electron equations of motion are

$$\frac{d\mathbf{r}^e}{dt} = \mathbf{v}^e \quad (3.13)$$

In $1 - D$ case (along x -axis only)

$$\frac{dx^e}{dt} = v_x^e \quad (3.14)$$

And

$$\frac{d\mathbf{v}^e}{dt} = \mathbf{a}^e \quad (3.15)$$

with component of accelerations

$$\frac{dv_x^e}{dt} = a_x^e \quad (3.16)$$

The macroscopic acceleration is

$$\mathbf{a}^e(\mathbf{r}) = -\frac{e}{m^e} [\mathbf{E}(\mathbf{r}) + \mathbf{v} \times \mathbf{B}(\mathbf{r})] \quad (3.17)$$

with its components

$$a_x^i = \frac{e}{m^e} [E(x) + (\mathbf{v} \times \mathbf{B}(\mathbf{r}))_x], \quad (3.18)$$

(b) Similarly, for the singly charged ions the velocity distribution functions satisfy the time independent Vlasov equations in differential form as

$$\frac{df^i}{dt} = \left[\mathbf{v} \cdot \frac{\partial}{\partial \mathbf{r}} + \frac{e}{m^i} (\mathbf{E}(\mathbf{r}) + \mathbf{v} \times \mathbf{B}(\mathbf{r})) \cdot \frac{\partial}{\partial \mathbf{v}} \right] f^i(\mathbf{r}, \mathbf{v}) \quad (3.19)$$

$$\equiv C^i \quad (3.20)$$

and in trajectory integrated forms as:

$$f^i(\mathbf{r}, \mathbf{v}) = f_{st}^i(\mathbf{r}_{st}^i, \mathbf{v}_{st}^i) + I^i(\mathbf{r}, \mathbf{v}) \quad (3.21)$$

where f_{st}^i is the “starting distribution”, \mathbf{r}_{st}^i is the starting configuration, \mathbf{v}_{st}^i is the starting velocity and I^i collision integral of ions. The ion equations of motion are

$$\frac{d\mathbf{r}^i}{dt} = \mathbf{v}^i \quad (3.22)$$

with components

$$\frac{dx^i}{dt} = v_x^i, \quad (3.23)$$

And

$$\frac{d\mathbf{v}^i}{dt} = \mathbf{a}^i \quad (3.24)$$

with component of acceleration

$$\frac{dv_x^i}{dt} = a_x^i, \quad (3.25)$$

The macroscopic acceleration is

$$\mathbf{a}^i(\mathbf{r}) = \frac{e}{m^e} [\mathbf{E}(\mathbf{r}) + \mathbf{v} \times \mathbf{B}(\mathbf{r})] \quad (3.26)$$

with its components

$$a_x^i = \frac{e}{m^e} [E(x) + (\mathbf{v} \times \mathbf{B}(\mathbf{r}))_x], \quad (3.27)$$

(c) The electric field is given by

$$\mathbf{E}(\mathbf{r}) = -\frac{d\phi(\mathbf{r})}{dr}, \quad (3.28)$$

where the electrostatic potential $\phi(\mathbf{r})$ is to be found from Poisson's equation

$$\frac{d^2\phi(\mathbf{r})}{dr^2} = -\frac{\rho(\mathbf{r})}{\epsilon_o}. \quad (3.29)$$

The space charge density is defined as

$$\rho(\mathbf{r}) = \sum_s q^s n^s(\mathbf{r}_j) \quad (3.30)$$

with the electron and ion densities given as

$$n^s(\mathbf{r}) = \int_{-\infty}^{\infty} d^3v f^s(\mathbf{r}, \mathbf{v}); \quad s = (e, i). \quad (3.31)$$

3.4 Boundary conditions

In the present case, the boundary potential, $\phi(\mathbf{r}_{st})$, and boundary injection distribution function, $f_{st}^s(\mathbf{r}_{st}, \mathbf{v}_{st})$, are assumed to be given. We choose $f_{st}^s(\mathbf{r}_{st}, \mathbf{v}_{st})$ such that the distribution function describes the physics we are interested in. Particularly, we assume the electron and ion velocity distribution functions to be cut-off Maxwellian in order to fulfill the most important requirements for presheath-sheath transition, i.e., quasi-neutrality, the sheath edge singularity condition, continuity of the first three moments of each species and the kinetic Bohm criterion. This model helps to obtain the distribution function at any point (\mathbf{r}, \mathbf{v}) of the phase space if the distribution function at any point in the simulation region is given.

Chapter 4

The Plasma Sheath Model

4.1 Description of the model

Our model consists of non-magnetized electrostatic plasma collisional sheath bounded by $x = 0$ and $x = L$ as shown in Fig. 4.1.

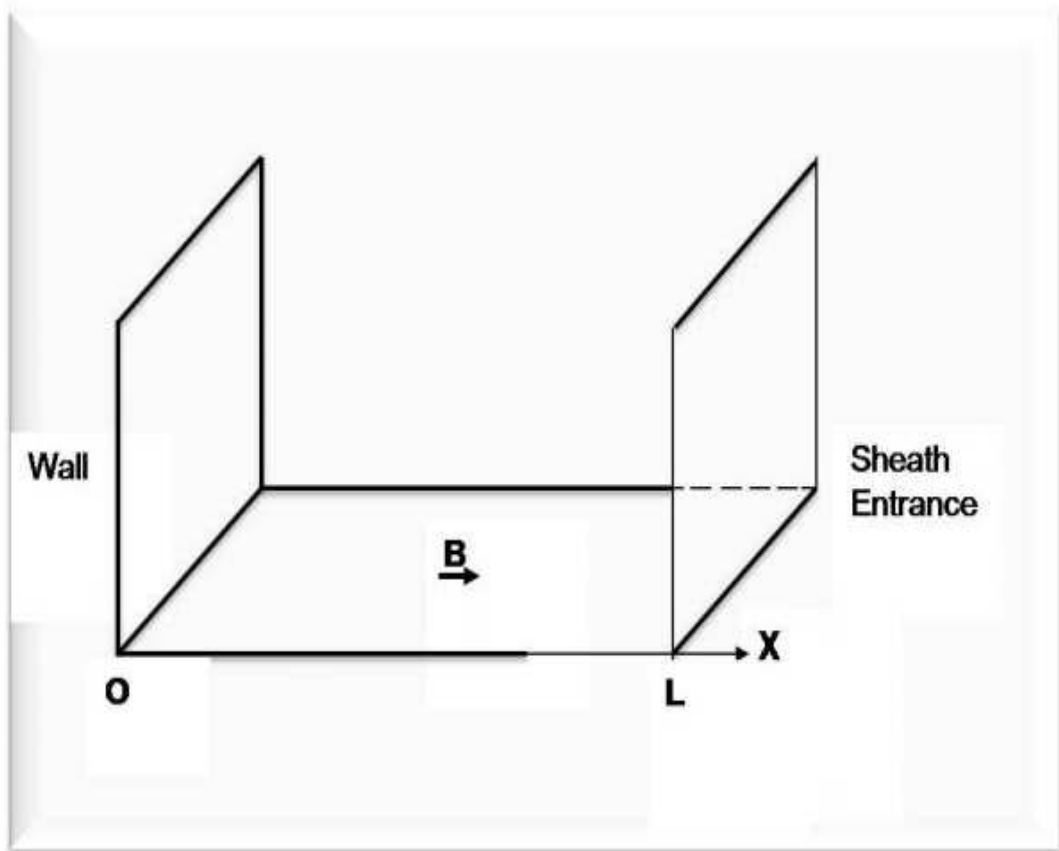


Figure 4.1: Plasma sheath model.

Plasma consists of only electrons and singly charged ions. The right hand boundary ($x = L$) is specified as the “sheath entrance” which separates the non neutral, collision sheath region ($x < L$) from the quasineutral, presheath region ($x > L$), whereas the left hand boundary ($x = 0$) represents an absorbing wall. We assume collision term such that collision integral

becomes

$$I^s = \alpha \frac{C_s L}{\lambda_D^2} \mathbf{v} \quad (4.1)$$

where $0 \leq \alpha \leq 1$ represents the degree of collision.

The value of α very over the range to study the sheath in different degree of collision. The value of α represents the degree of collision, i.e. how frequent the collision occur. Lets take $\alpha = 0.01$ which implies that if a particle encounters 100 other particles it undergoes a single collision, $\alpha = 1$ corresponds to the case where every encounter is collision . The $\alpha = 0$ represents the collisionless case and $0 < \alpha \leq 1$ represents the collisional cases. The $\alpha = 1$ represents fully collisional sheath which is not practically possible. The sheath is almost collisionless so it is suitable to take smaller value of α close to 0.

4.2 Boundary conditions

To solve the set of equations compiled in Section 3.3, we need to know the boundary conditions for the velocity distribution functions (particle boundary condition) and the potential (field boundary condition) at the two boundaries of the simulation region. The boundary potentials, $\phi(x = 0)$ and $\phi(x = L)$, the boundary injection distribution function, $f^s(L, \mathbf{v})$ and the distribution function at the wall, $f^s(0, \mathbf{v})$, are assumed to be given. Hence, they must be specified before the iteration is started and are kept constant throughout the entire simulation.

(a) Particle boundary conditions

We assume here the plasma particle enters the simulation region from the right hand boundary with cut off Maxwellian velocity distributions functions, the left hand boundary does not emit any particle and that both boundaries are perfectly absorbing. Due to this, the distribution function satisfies the following boundary conditions:

at the left hand boundary,

$$f^s(x = 0, \mathbf{v} \geq 0) = 0; \quad s = (e, i). \quad (4.2)$$

At the right hand boundary,

$$\begin{aligned} f^e(x = L, \mathbf{v} \leq 0) &= A^e \exp \left[-\frac{m^e v^2}{2k_B T^e} \right] \\ &= A^e \exp \left[-\left(\frac{\mathbf{v}}{\mathbf{v}_{tf}^e} \right)^2 \right], \end{aligned} \quad (4.3)$$

and

$$\begin{aligned} f^i(x = L, \mathbf{v} \leq 0) &= A^i \exp \left[-\frac{m^i (\mathbf{v} - \mathbf{v}_{mL}^i)^2}{2k_B T^i} \right] \Theta(v_{cL}^i - v_x) \\ &= A^i \exp \left[-\left(\frac{\mathbf{v} - \mathbf{v}_{mL}^i}{\mathbf{v}_{tf}^i} \right)^2 \right] \Theta(v_{cL}^i - v_x), \end{aligned} \quad (4.4)$$

where T^e and T^i are the electron and ion formal temperatures respectively. The thermal velocity of species 's' is given by

$$\mathbf{v}_{tf}^s = \sqrt{\frac{2k_B T^s}{m^s}}, \quad (4.5)$$

where \mathbf{v}_{mL}^i is the ion "Maxwellian-maximum" velocity at $x = L$ and \mathbf{v}_{cL}^i ($\mathbf{v}_{cL}^i < 0$) is the ion cut-off velocity at $x = L$. We assume the particles enter the injection plane with half Maxwellian and our potential profile is monotonically decreasing towards the left hand boundary. Together with these two conditions the total electron velocity distribution function is given by

$$f^e(x = L, \mathbf{v} \leq 0) = A^e \exp \left[-\frac{v^2}{v_{tf}^e} + \frac{e\phi(x)}{k_B T_f^e} \right] \Theta(v_{cL}^e - v_x), \quad (4.6)$$

where

$$v_{cL}^e = \sqrt{\frac{2e[\phi(x) - \phi_o]}{m^e}} \quad (4.7)$$

is the electron cut-off velocity at point x . For $x = L$, we have

$$f^e(x = L, \mathbf{v}) = A^e \exp \left[-\left(\frac{v^2}{v_{tf}^e} \right) \right] \Theta(v_{cL}^e - v_x), \quad (4.8)$$

where

$$v_{cL}^e = \sqrt{\frac{-2e\phi_o}{m^e}}. \quad (4.9)$$

Similarly, for the ions from Eq. (4.4) and using the fact that our potential profile is monotonically decreasing towards the wall (left hand boundary) and ions enter the sheath entrance with half Maxwellian velocity distribution function gives the total velocity distribution function for ions at $x = L$ is

$$f^i(x = L, \mathbf{v}) = A^i \exp \left[- \left(\frac{\mathbf{v} - \mathbf{v}_{mL}^i}{v_{tf}^i} \right)^2 \right] \Theta(v_{cL}^i - v_x). \quad (4.10)$$

In the right hand side of the Eq. (4.8) and Eq. (4.10), there are seven parameters $A^e, T_f^e, v_{cL}^e, A^i, T_f^i, v_{mL}^i$ and v_{cL}^i which must be specified according to the physical situation considered.

Now the particle density and other physical parameters at $x = L$ are given by

$$n_L^s = \int_{-\infty}^{+\infty} dv f^s(L, \mathbf{v}). \quad (4.11)$$

The average or fluid velocity,

$$\begin{aligned} u_L^s &= \langle v \rangle_L^s \\ &= \int_{-\infty}^{+\infty} dv v f^s(L, \mathbf{v}) \end{aligned} \quad (4.12)$$

and effective temperature,

$$T_{eff,L}^s = \frac{2}{k} \left\langle \frac{m^s(v - u)^2}{2} \right\rangle_L \quad (4.13)$$

The electron density at $x = L$ is calculated with Eq. (4.11), (4.8)

$$\begin{aligned} n_L^e &= \int_{-\infty}^{\infty} dv f^e(L, \mathbf{v}) \\ &= A^e \int_{-\infty}^{\infty} dv \exp \left[- \left(\frac{v}{v_{tf}^e} \right)^2 \right] \Theta[v_{cL}^e - v] \\ &= A^e \int_{-\infty}^{v_{cL}^e} dv \exp \left[- \left(\frac{v}{v_{tf}^e} \right)^2 \right] \end{aligned}$$

using $\left(\frac{v}{v_{tf}^e}\right) = \xi$, we get

$$\begin{aligned} n_L^e &= A^e \int_{-\infty}^{\frac{v_{cL}^e}{v_{tf}^e}} v_{tf}^e \exp(-\xi^2) d\xi \\ &= A^e v_{tf}^e \left[\frac{\sqrt{\pi}}{2} + \frac{\sqrt{\pi}}{2} \operatorname{erf}\left(\frac{v_{cL}^e}{v_{tf}^e}\right) \right] \\ &= \frac{A^e \pi^{1/2} v_{tf}^e}{2} C^e, \end{aligned} \quad (4.14)$$

where

$$\begin{aligned} C^e(T_f^e, \phi_o) &= 1 + \operatorname{erf}\left(\frac{v_{cL}^e}{v_{tf}^e}\right) \\ &= 1 + \operatorname{erf}\sqrt{\frac{-e\phi_o}{k_B T_f^e}}. \end{aligned} \quad (4.15)$$

We define “erf” as “Error function”, which is given by

$$\operatorname{erf}(x) = \frac{2}{\sqrt{\pi}} \int_0^x d\xi \exp(-\xi^2). \quad (4.16)$$

Now, from the velocity distribution function Eq. (4.10) and Eq. (4.11) we get ion density as

$$\begin{aligned} n_L^i &= \int_{-\infty}^{+\infty} dv f^i(L, \mathbf{v}) \\ &= \int_{-\infty}^{+\infty} dv A^i \exp\left[-\left(\frac{\mathbf{v} - \mathbf{v}_{mL}^i}{\mathbf{v}_{tf}^i}\right)^2\right] \Theta[v_{cL}^i - v_x] \\ &= A^i \int_{-\infty}^{v_{cL}^i} dv \left[-\left(\frac{(v_x - v_{mL}^i)}{v_{tf}^i}\right)^2\right] \end{aligned}$$

using $\left(\frac{v - v_{mL}^i}{v_{tf}^i}\right) = \xi$, we get

$$\begin{aligned} n_L^i &= A^i \int_{-\infty}^{(v_{cL}^i - v_{mL}^i)/v_{tf}^i} v_{tf}^i \exp(-\xi^2) d\xi \\ &= A^i v_{tf}^i \left[\frac{\sqrt{\pi}}{2} + \frac{\sqrt{\pi}}{2} \operatorname{erf}\left(\frac{v_{cL}^i - v_{mL}^i}{v_{tf}^i}\right) \right] \\ &= \frac{A^i \pi^{1/2} v_{tf}^i}{2} [1 + \operatorname{erf}(\tau_{cL}^i)] \\ &= \frac{A^i \pi^{1/2} v_{tf}^i}{2} C^i, \end{aligned} \quad (4.17)$$

where $C^i = 1 + \text{erf}(\tau_{cL}^i)$ and $\tau_{cL}^i = \left(\frac{v_{cL}^i - v_{mL}^i}{v_{tf}^i} \right)$. We can also define the “complementary error function” as

$$\text{erfc}(x) = 1 - \text{erf}(x). \quad (4.18)$$

The average electron velocity is calculated with help of Eq. (4.8), (4.14), (4.12)

$$\begin{aligned} u_L^e &= \frac{1}{n_L^e} \int_{-\infty}^{+\infty} dv v f^e(L, v) \\ &= -\frac{v_{tf}^e D^e}{\pi^{1/2} C^e} \end{aligned} \quad (4.19)$$

where,

$$\begin{aligned} D^e(T_f^e, \phi_0) &= \exp\left[-\frac{v_{cL}^e}{v_{tf}^e}\right] \\ &= \exp\left[-\frac{e\phi_0}{kT_f^e}\right] \end{aligned} \quad (4.20)$$

The ion average velocity is given by Eq. (4.10), (4.17), (4.12)

$$\begin{aligned} u_L^i &= \frac{1}{n_L^i} \int_{-\infty}^{+\infty} dv v f^i(L, v) \\ &= v_{mL}^i - \frac{v_{tf}^i D^i}{\pi^{1/2} C^i} \end{aligned} \quad (4.21)$$

where,

$$\begin{aligned} D^i(T_f^i) &= \exp\left[-\left(\frac{v_{cL}^i - v_{mL}^i}{v_{tf}^i}\right)^2\right] \\ &= \exp[-\tau^2] \end{aligned} \quad (4.22)$$

The electron effective temperature is given by Eq. (4.8), (4.14), (4.13), (4.19)

$$\begin{aligned} T_{eff,L}^e &= \frac{m^e}{kn_L^e} \int_{-\infty}^{+\infty} dv (v - u_L^e)^2 f^e(L, v) \\ &= T_f^e [1 - \frac{2v_{cL}^e D^e}{\pi^{1/2} v_{tf}^e C^e} - \frac{2}{\pi} (\frac{C^e}{D^e})^2] \end{aligned} \quad (4.23)$$

where,

$$T_f^e = \frac{m^e v_{tf}^e}{2k} \quad (4.24)$$

The ion effective temperature is given by Eq. (4.10), (4.17), (4.13), (4.21)

$$\begin{aligned} T_{eff,L}^i &= \frac{m^i}{kn_L^i} \int_{-\infty}^{+\infty} dv (v - u_L^i)^2 f^i(L, v) \\ &= T_f^i [1 - \frac{2\tau_{cL}^i D^i}{\pi^{1/2} C^i} - \frac{2}{\pi} (\frac{D^i}{C^i})^2] \end{aligned} \quad (4.25)$$

where,

$$T_f^i = \frac{m^i v_{tf}^i}{2k} \quad (4.26)$$

(b) Field boundary conditions

The potential profile at $x = L$ is chosen as zero, whereas the one at $x = 0$ is fixed to a negative constant value, i.e.

$$\phi(x = 0) = \phi_o \text{ (constant)} < 0 \quad (4.27)$$

$$\begin{aligned} \phi(x = L) &= \phi(L) \\ &= 0. \end{aligned} \quad (4.28)$$

We restrict ourselves to the potential distribution which decreases monotonically from $x = L$ to $x = 0$ such that the electric field is always negative as shown in Fig. 4.2.

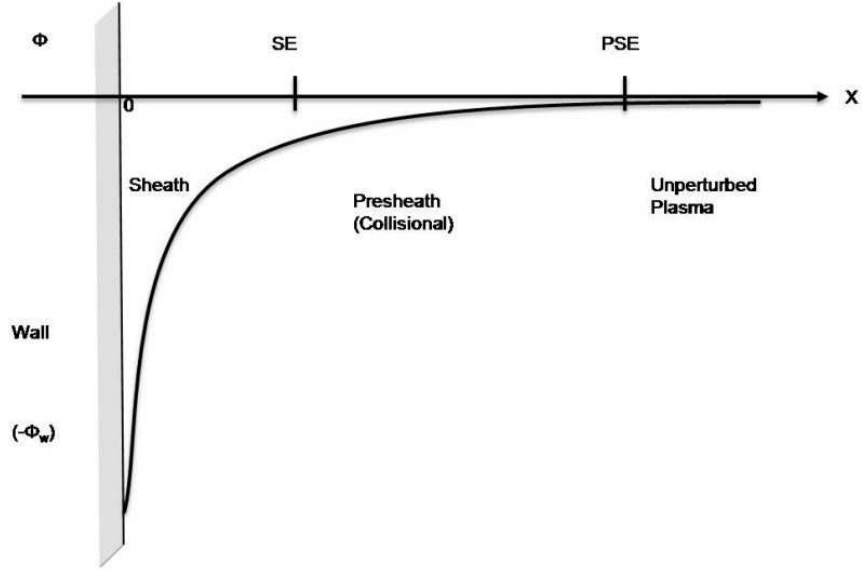


Figure 4.2: Example of potential profile decreasing monotonically from $x = L$ towards $x = 0$.

4.3 Bohm criterion

In order to form sheath the ions at sheath entrance must have a velocity greater or equal ion acoustic velocity which was shown by Bohm and known as “Bohm Criterion”. Here we derive Bohm criterion [7, 19], which is satisfied by injected ion velocity distribution function, so that formation of sheath is possible, whereas the electron distribution is assumed to satisfy full Maxwellian.

We have the Poisson’s equation

$$\frac{d^2\phi}{dx^2} = -\frac{\rho(\phi)}{\epsilon_0}. \quad (4.29)$$

Expanding the above equation in Taylor’ series about $x \approx L$, we get

$$\left[\frac{d^2\phi}{dx^2} \right]_{x \rightarrow L} = -\frac{1}{\epsilon_0} \left[\rho(\phi_L) + \phi \left[\frac{d\rho}{d\phi} \right]_{x \rightarrow L} + \frac{\phi^2}{2} \left[\frac{d^2\rho}{d\phi^2} \right]_{x \rightarrow L} + \dots \right]. \quad (4.30)$$

As we have assumed at the sheath entrance the plasma is quasineutral, i.e. $\rho(x_L) = 0$, $n_{ps}^i = n_{ps}^e$. Hence, using the quasineutrality condition and neglecting second and higher order

terms from Eq. (4.30), we obtain

$$\left[\frac{d^2\phi}{dx^2} \right]_{x \rightarrow L} + \frac{\phi}{\epsilon_0} \left[\frac{d\rho}{d\phi} \right]_{x \rightarrow L} = 0. \quad (4.31)$$

But we have taken potential profile monotonically decreasing towards the wall i.e., of the form $\phi(x \leq L) \leq 0$. Hence the Eq. (4.31) will have non-oscillatory solution only if

$$\left[\frac{d\rho}{d\phi} \right]_{x \rightarrow L} \leq 0. \quad (4.32)$$

The above relation can also be expressed in terms of particle densities as

$$\left[\frac{d\rho}{d\phi} \right]_{x \rightarrow L} = e \left[\frac{dn^i}{d\phi} - \frac{dn^e}{d\phi} \right]_{x \rightarrow L}. \quad (4.33)$$

The electron density including the potential profile at any point is given by

$$n^e(\phi) = n_L^e \exp \left[\frac{e\phi}{k_B T_f^e} \right] \left[\frac{1 + \operatorname{erf} \sqrt{\frac{e(\phi - \phi_o)}{k_B T_f^e}}}{1 + \operatorname{erf} \sqrt{\frac{-e\phi_o}{k_B T_f^e}}} \right]. \quad (4.34)$$

Differentiating the above equation with respect to ϕ yields

$$\frac{dn^e(\phi)}{d\phi} = \frac{n_L^e e}{k_B T_f^e} \exp \left[\frac{e\phi}{k_B T_f^e} \right] \left[\frac{1 + \operatorname{erf} \sqrt{\frac{e(\phi - \phi_o)}{k_B T_f^e}}}{1 + \operatorname{erf} \sqrt{\frac{-e\phi_o}{k_B T_f^e}}} \right] + \frac{n_L^e e}{k_B T_f^e} \exp \left[\frac{e\phi_o}{k_B T_f^e} \right] \frac{\sqrt{\frac{k_B T_f^e}{e\pi(\phi - \phi_o)}}}{1 + \operatorname{erf} \sqrt{\frac{-e\phi_o}{k_B T_f^e}}}. \quad (4.35)$$

But at $x \rightarrow L$, $\phi \rightarrow 0$, Eq. (4.35) reduces to

$$\left[\frac{dn^e(\phi)}{d\phi} \right]_{x \rightarrow L} = \frac{n_L^e e}{k_B T_f^e} \left[1 + \exp \left[\frac{e\phi_o}{k_B T_f^e} \right] \frac{\sqrt{\frac{-k_B T_f^e}{e\pi(\phi_o)}}}{1 + \operatorname{erf} \sqrt{\frac{-e\phi_o}{k_B T_f^e}}} \right]. \quad (4.36)$$

The ion density at any point x is given by

$$n^i(\phi) = \int_{-\infty}^{v_{cL}^i} dv \left[1 - \frac{2e\phi}{m^i v^2} \right]^{\frac{-1}{2}} f_L^i(v). \quad (4.37)$$

After differentiating the Eq. (4.38) we get

$$\frac{dn^i(\phi)}{d\phi} = \int_{-\infty}^{v_{cL}^i} dv \frac{f_L^i(v)}{v^2} \left[1 - \frac{2e\phi}{m^i v^2} \right]^{\frac{3}{2}}. \quad (4.38)$$

As $2e\phi < m^i v^2$ at $x \approx L$, we can expand above equation to get

$$\left[\frac{dn^i}{d\phi} \right]_{x \rightarrow L} = \frac{e}{m^i} \int_{-\infty}^{v_{cL}^i} dv \frac{f_L^i(v)}{v^2} \left[1 + \frac{3e\phi}{m^i v^2} \right]. \quad (4.39)$$

At $x \approx L$

$$\left[\frac{dn^i}{d\phi} \right]_{x \rightarrow L} \equiv \frac{e}{m^i} \int_{-\infty}^{v_{cL}^i} dv \frac{f_L^i(v)}{v^2}. \quad (4.40)$$

From Eq. (4.33), (4.36) and (4.40) we get

$$\left[\frac{d\rho}{d\phi} \right]_{x \rightarrow L} = e^2 \left[\frac{1}{m^i} \int_{-\infty}^{v_{cL}^i} dv \frac{f_L^i(v)}{v^2} - \frac{n_L^e}{k_B T_f^e} \left(1 + \sqrt{\frac{-k_B T_f^e}{e\pi\phi_o}} \frac{\exp\left(\frac{e\phi_o}{k_B T_f^e}\right)}{1 + \operatorname{erf}\sqrt{\frac{-e\phi_o}{k_B T_f^e}}} \right) \right]. \quad (4.41)$$

Then we can write,

$$\left\langle \frac{1}{v^2} \right\rangle_L^i \leq \frac{1}{C_s^2} \left[1 + \sqrt{\frac{-k_B T_f^e}{e\pi\phi_o}} \frac{\exp\left(\frac{e\phi_o}{k_B T_f^e}\right)}{1 + \operatorname{erf}\sqrt{\frac{-e\phi_o}{k_B T_f^e}}} \right], \quad (4.42)$$

where

$$\left\langle \frac{1}{v^2} \right\rangle_L^i \leq \frac{1}{n_L} \int_{-\infty}^{v_{cL}^i} dv \frac{f_L^i(v)}{v^2} \quad (4.43)$$

and

$$C_s^2 = \frac{k_B T_f^e}{m^i}. \quad (4.44)$$

C_s is ion acoustic velocity.

4.4 Presheath-sheath approximation

The plasma flowing towards the wall passes through the two regions: the narrow region in which there is large gradient of electric field and supersonic velocity called “sheath”, and the region attached with the bulk plasma with relatively weak gradient of variables and in general subsonic flow is called “presheath” [20].

The scale length of the sheath and presheath is different. So usually they are studied separately using different models and methods [6]. For our case, to couple the different solutions at the presheath and sheath side is important.

we have applied the coupling scheme [16], which gives the plasma parameters at the sheath side of the sheath entrance for parameters given at the presheath side. This coupling scheme satisfies the most crucial requirement of the presheath-sheath transition, i.e. quasi-neutrality, the sheath edge singularity condition and kinetic “Bohm-Chodura criterion”.

4.4.1 Presheath

We assume that the parameters at the presheath side of the sheath region are given or can be obtained by velocity distribution function. Let us assume the ion and electron densities, n_{ps}^i and n_{ps}^e , the fluid velocities, u_{ps}^i and u_{ps}^e , and the temperatures T_{ps}^i and T_{ps}^e ; at the presheath side of the sheath-presheath boundary (characterized by $x = L$). These six parameters are not completely independent but are related by the quasineutrality condition

$$n_{ps}^e = n_{ps}^i \quad (4.45)$$

and the sheath edge singularity condition

$$u_{ps}^i = -C_s, \quad (4.46)$$

where

$$C_s = \sqrt{\frac{k_B (\gamma^i T_{ps}^i + \gamma^e T_{ps}^e)}{m^i}}. \quad (4.47)$$

Also the electric current density at presheath region is defined by

$$j_{ps} = e (n_{ps}^i u_{ps}^i - n_{ps}^e u_{ps}^e) \quad (4.48)$$

and at the presheath region

$$n_{ps}^e = n_{ps}^i = n_{ps}. \quad (4.49)$$

In summary, at the sheath edge ($x = L$) our two fluid presheath plasma is characterized by nine parameters, n_{ps}^e , n_{ps}^i , n_{ps} , u_{ps}^i , u_{ps}^e , T_{ps}^i , T_{ps}^e , C_s and j_{ps} , which are related by conditions

(4.45)-(4.49) so that knowing four of them we obtain the remaining five.

4.4.2 Sheath

The electron and ion distribution function at $x = L$ describing the sheath are given by Eq. (4.8) and Eq. (4.10) respectively and first three moments are calculated from Eq. (4.14), Eq. (4.19) and Eq. (4.23), for electron and from Eq. (4.17), Eq. (4.21) and Eq. (4.25) for ion respectively.

The seven sheath parameters indicated in sec. 4.2(a) are no independent of other but are interrelated by two boundary condition at $x = L$, namely quasineutrality condition

$$n_L^e(A^e, T_f^e, \phi_o) = n_L^i(A^i, T_f^i, v_{mL}^i, v_{cL}^i) \quad (4.50)$$

and the Bohm Criterion,

$$\int_{-\infty}^{v_{cL}^i} \frac{dv}{v^2} \exp\left[-\frac{m^i(v - v_{mL}^i)^2}{2kT_f^i}\right] = \frac{n_L^e m^i}{kT_f^e A^i} \left(1 + \sqrt{\frac{-kT_f^e}{e\pi\phi_o} \frac{D^e}{C^e}}\right) \quad (4.51)$$

Hence, prescribing five of seven parameters will fix the remaining two, Eq. (4.50) and (4.51), following from the Bohm criterion.

4.4.3 Presheath-Sheath coupling

Now, we need to couple our kinetic sheath solution $x = L_-$ to the fluid presheath solution at $x = L_+$. For this, we require the sheath side particle density, n_L^s fluid velocity, u_L^s , and effective temperature, $T_{eff,L}^s$ respectively to be equal their presheath side counterparts, n_{ps} , u_{ps} , and T_{ps} .

Equating these values taken from presheath counterparts, we obtain,

$$n_{ps}^e = \sqrt{\frac{\pi k T_f^e}{2m^e}} C^e A^e \quad (4.52)$$

$$u_{ps}^e = -\sqrt{\frac{\pi k T_f^e}{\pi m^e}} \frac{D^e}{C^e} \quad (4.53)$$

$$T_{ps}^e = T_f^e \left[1 - \sqrt{-\frac{4e\phi_o}{\pi k T_f^e}} \frac{D^e}{C^e} - \frac{2}{\pi} \left(\frac{C^e}{D^e} \right)^2 \right] \quad (4.54)$$

$$n_{ps}^i = \sqrt{\frac{\pi k T_f^i}{2m^i}} C^i A^i \quad (4.55)$$

$$u_{ps}^i = v_{mL}^i - \sqrt{\frac{2k T_f^i}{\pi m^i}} \frac{D^i}{C^i} \quad (4.56)$$

and

$$T_{ps}^i = T_f^i \left[1 - \sqrt{\frac{2m^i}{\pi T_f^i}} \frac{D^i}{C^i} (v_{cL}^i - v_{mL}^i) - \frac{2}{\pi} \left(\frac{D^i}{C^i} \right)^2 \right] \quad (4.57)$$

Hence, we have seen equations, Eq. (4.51) and Eq. (4.52-4.57), which permit us to express seven sheath parameters A^e , T_f^e , ϕ_o , A^i , T_f^i , v_{mL}^i and v_{cL}^i in terms of five presheath parameters, n_{ps} , u_{ps}^e , T_{ps}^e , u_{ps}^i and T_{ps}^i .

Thus, for given presheath parameters the correspondinfg sheath parameters can be obtained by solving these equations.

Chapter 5

Numerical Method

5.1 Discretization of the simulation region

Our simulation region $x = 0$ and $x = L$, is discretized uniformly in configuration and velocity space as shown in Fig. 5.1.

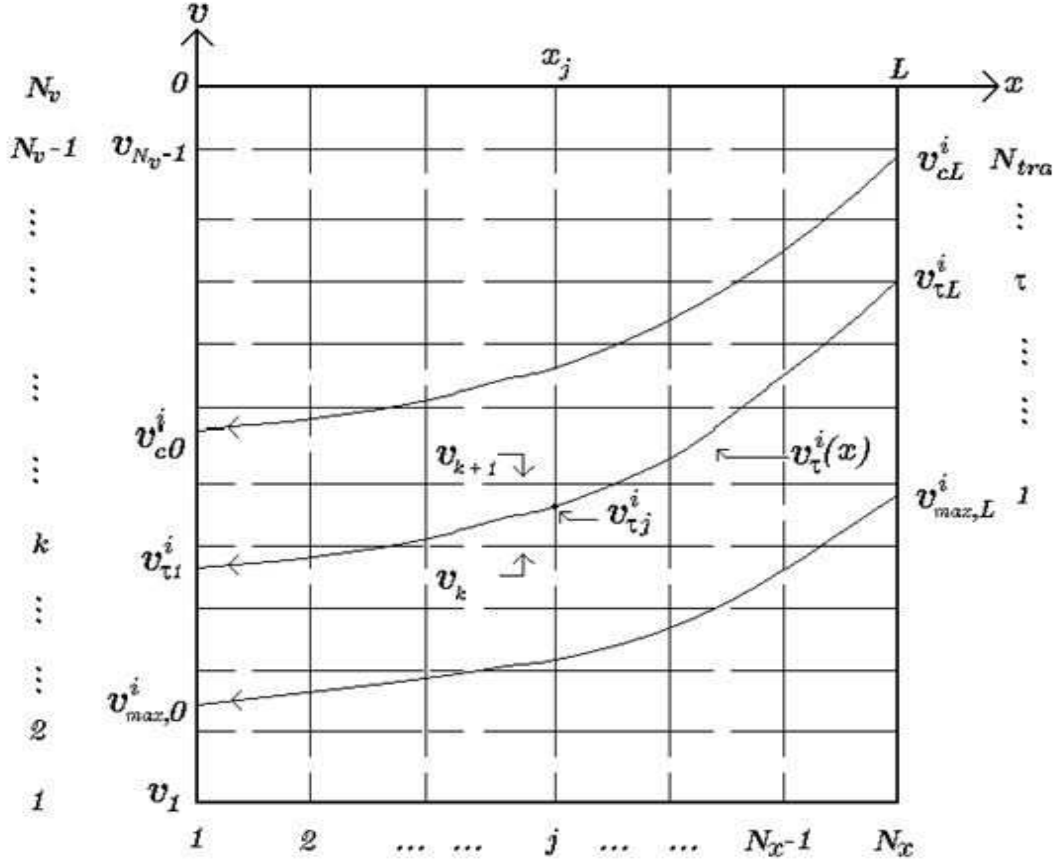


Figure 5.1: Schematic representation of the phase-space gridding. The vertical and horizontal dashed lines respectively represent the position and velocity grids.

In Fig. 5.1 the position grid point is denoted as x_j ($j = 1, 2, 3, \dots, n_x$), with n_x the total number of grid points, and the separation between consecutive grid points is denoted by Δx . In our discretization, $j = 1$ and $j = n_x$ respectively correspond to the left-hand boundary ($x = 0$) and the right-hand boundary ($x = L$). In our simulation we choose n_x such that the

grid size is always less than the Debye length of the injected electrons

$$\lambda_D^e = \sqrt{\frac{\epsilon_0 k_B T^e}{e^2 n_L^e}}. \quad (5.1)$$

If we are interested to estimate the values of any quantity that we required in simulation region we use method of interpolation. Let the value of any quantity $Q(x)$ at the grid points are denoted as $Q_j = Q(x_j)$, its value at any point ‘ x ’ between two grid points Q_j and Q_{j+1} can be approximated by means of linear interpolation approximation method

$$Q(x) = \left(\frac{x_{j+1} - x}{\Delta x} \right) Q_j + \left(\frac{x - x_j}{\Delta x} \right) Q_{j+1}, \quad (5.2)$$

where $x_j < x < x_{j+1}$.

Another standard approximation is the second-order interpolation between the points x_{j-1} and x_{j+1} is

$$Q(x) = Q_j + a(x - x_j) + b(x - x_j)^2, \quad (5.3)$$

at point $x = x_{j-1}$ is

$$Q_{j-1} = Q_j - a\Delta x + b(\Delta x)^2 \quad (5.4)$$

and at points $x = x_{j+1}$ is

$$Q_{j+1} = Q_j + a\Delta x + b(\Delta x)^2. \quad (5.5)$$

From Eq. (5.4)

$$a = \left(\frac{Q_j - Q_{j-1} + b(\Delta x)^2}{\Delta x} \right). \quad (5.6)$$

Putting the value of ‘ a ’ in Eq. (5.5), we get

$$Q_{j+1} = Q_j + [Q_j - Q_{j-1} + b(\Delta x)^2] \quad (5.7)$$

Solving above equation

$$b = \left(\frac{Q_{j+1} + Q_{j-1} - 2Q_j}{2(\Delta x)^2} \right). \quad (5.8)$$

Using this value of ‘ b ’, we get value of ‘ a ’ as

$$a = \left(\frac{Q_{j+1} - Q_{j-1}}{2\Delta x} \right). \quad (5.9)$$

Putting the value of ‘ a ’ and ‘ b ’ in Eq. (5.3)

$$Q(x) = Q_j + (x - x_j) \left(\frac{Q_{j+1} - Q_{j-1}}{2\Delta x} \right) + \frac{1}{2}(x - x_j)^2 \left(\frac{Q_{j+1} + Q_{j-1} - 2Q_j}{(\Delta x)^2} \right). \quad (5.10)$$

The Taylor series expansion about x_0 is

$$Q(x) = Q(x_0) + (x - x_0)Q'(x_0) + \frac{(x - x_0)^2}{2!}Q''(x_0) + \dots \quad (5.11)$$

Comparing Eq. (5.10) with Eq. (5.11), the first and second derivatives of any quantity $Q(x)$ are approximated respectively as,

$$\left(\frac{dQ}{dx} \right)_j = \left(\frac{Q_{j+1} - Q_{j-1}}{2\Delta x} \right) \quad (5.12)$$

and

$$\left(\frac{d^2Q}{dx^2} \right)_j = \left(\frac{Q_{j+1} + Q_{j-1} - 2Q_j}{(\Delta x)^2} \right) \quad (5.13)$$

5.2 Electron density distribution

In simulation region the electron density calculated analytically. The electron density at some grid point x_j is obtained by using the electron distribution function in the expression for particle density Eq. (4.11). In order to obtain the electron density profile at any point x we require potential $\phi(x)$ to be known. In our calculation, we obtain the electron density at the grid point x_j in terms of potential as

$$n_j^e = n_L^e \exp \left(\frac{e\phi_j}{k_B T_f^e} \right) \left[1 + \operatorname{erf} \sqrt{\frac{e(\phi_j - \phi_0)}{k_B T_f^e}} \right], \quad (5.14)$$

where $n_j^e = n^e(x_j)$ and $\phi_j = \phi(x_j)$.

With the help of Eq. (5.14) electron density at any point in simulation region can be obtained if once we know the value of potential at that point.

5.3 Discretizing ion velocity space with a fixed grid

As in the Fig. (5.1), the ion velocity space is discretized uniformly with n_v the total number of velocity grid points and the k^{th} ion velocity grid value being denoted as v_k ($k = 1, 2, 3, \dots, n_v$). In our discretization $k = 1$ and $k = n_v$ respectively corresponds to the fastest and the slowest ion velocities taken into account. Since in our simulation scheme only ions with negative velocities are considered, we set $v_{n_v} = 0$ and choose $|v_1|$ sufficiently large such that the velocity of the fastest ion reaching the left-hand boundary does not exceed this value, i.e. $|v_1| \geq |v_{max,0}^i|$. In our case we choose n_v to be large enough for the velocity grid size to always be considerably less than the ion thermal velocity v_{tf}^i .

5.4 Ion trajectories

5.4.1 Discrete set of the injection velocities

In our simulation region the ions are injected at the right-hand boundary i.e at $x = L$ in the velocity range $-\infty < v \leq v_{cL}^i$. In our numerical implementation, we approximate this domain by the finite $v_{max,L}^i \leq v \leq v_{cL}^i$ and discretize the velocity domain with n_{tra} equidistant ion injection velocities $v_{\tau L}^i$ ($\tau = 1, 2, \dots, n_{tra}$), where $\tau = 1$ and $\tau = n_{tra}$ respectively corresponds to the injection velocities $v_{max,L}^i$ and v_{cL}^i . Choice of v_{cL}^i depends on the problem considered and the maximum injection velocity $v_{max,L}^i$ is chosen sufficiently large for the ion distribution function corresponding to velocities larger than this velocity to be negligible. In our computations, we use $v_{max,L}^i = v_{cL}^i - 4v_{tf}^i$, where v_{tf}^i is the ion thermal velocity.

5.4.2 Discrete set of ion trajectories

The ion injection velocity in the simulation region at right hand boundary ($x = L$) represents the starting velocity of a collisionless ion trajectory, the n_{tra} discrete injection velocities $v_{\tau L}^i$

define n_τ related trajectories labeled by the index τ . We denote the trajectory corresponding to some injection velocity $v_{\tau L}^i$ by $v_\tau^i(L)$, and the velocity with which it crosses a grid point x_j is $v_{\tau j}^i = v_\tau^i(x_j)$, so that $v_{\tau n_x}^i \cong v_{\tau L}^i = v_\tau^i(L)$ in phase space. The velocities v_τ^i represents the intersections of ion trajectories $v = v_{tau}^i(x)$ and spatial grid lines $x = x_j$, which is said to be “intersection velocities”. The ion injection velocities $v_{\tau L}^i$ are independent of the ion grid velocities v_k , but in practice we will often choose them such that each $v_{\tau L}^i$ coincide with one of the v_k ’s.

5.4.3 Numerical calculation of ion trajectories

In the KTS method we trace the collisionless trajectories to calculate the related velocity distribution functions along them. In this section we consider only ion trajectories and hence omit the species index ‘i’. For the calculation of the ion trajectory, we simply discretize the ion equation of motion Eq. (3.13) and Eq. (3.17) in a time-centered manner as

$$\frac{x^{m+\frac{1}{2}} - x^{m-\frac{1}{2}}}{\Delta t} = v_x^m. \quad (5.15)$$

For change in v_x

$$\begin{aligned} \frac{v_x^m - v_x^{m-1}}{\Delta t} &= a_x^{m-\frac{1}{2}} \\ &= \frac{e}{m^i} \left[E \left(x^{m-\frac{1}{2}} \right) + (\mathbf{v} \times \mathbf{B})_x^{m-\frac{1}{2}} \right] \\ &= \frac{e}{m^i} E \left(x^{m-\frac{1}{2}} \right) \end{aligned} \quad (5.16)$$

Where we use Δt is the numerical time-step size and $m \geq 0$ is an integral or half integral superscript, i.e. $v^m = v(t^m)$, $x^{m+\frac{1}{2}} = x(t^{m+\frac{1}{2}})$, etc. This corresponds to the total time elapsed in steps of Δt for an ion having been injected at time zero at the right-hand boundary.

So, $m = 0$ corresponds to $t = 0$ with the injection (or starting) values

$$x^0 = L \quad (5.17)$$

and

$$v_x^0 = v_{\tau L}^i. \quad (5.18)$$

The choice of positions at half integral times and velocity at integral times in Eq. (5.15) and (5.16) makes the numerical scheme time centered. For any time step $m \geq 1$, with $x^{m-\frac{1}{2}}$ and v^{m-1} being given from the $(m-1)^{st}$ step, we calculate the new ion velocity from Eq. (5.16) as

$$v_x^m = v_x^{m-1} + \frac{e\Delta t}{m^i} E(x^{m-\frac{1}{2}}) \quad (5.19)$$

and we can also find new position of the ions from Eq. (5.15)

$$x^{m+\frac{1}{2}} = x^{m-\frac{1}{2}} + \Delta t v_x^m. \quad (5.20)$$

The electric field $E(x)$ in equation (5.19) at any point in the simulation region is obtained by the relation (3.28). Thus the numerical scheme ends up with x-points at half-integral times $(x^{m+\frac{1}{2}})$ and velocities at integral times (v_x^m) along a collisionless trajectory. We can also find the ion velocity at $x^{m+\frac{1}{2}}$ by the relation

$$v_x^{m+\frac{1}{2}} = \frac{v_x^m + v_x^{m+1}}{2}. \quad (5.21)$$

5.4.4 Intersection velocities

The velocities at half integral time as in Eq. (5.21) may not coincide with our fixed grid points x_j . For the calculation of the intersection velocities for the τ^{th} trajectory at some inner grid point x_j the linear interpolation can be used as

$$v_{\tau j}^i = \frac{\left(x^{m-\frac{1}{2}} - x_j\right) v_x^{m+\frac{1}{2}} + \left(x_j - x^{m+\frac{1}{2}}\right) v_x^{m-\frac{1}{2}}}{\left(x^{m-\frac{1}{2}} - x^{m+\frac{1}{2}}\right)}, \quad (5.22)$$

where $x^{m-\frac{1}{2}}$ and $x^{m+\frac{1}{2}}$ are the adjacent points along the trajectory on the right-hand side and the left-hand side of the grid point x_j , respectively. In order to calculate the ion velocity at the left-hand boundary ($x=0$) we use a parabolic extrapolation scheme. For this considering

the last three calculated points along the trajectory which lie to the right-hand side of the left-hand boundary $\left[\left(x^{m-\frac{1}{2}}, v_x^{m-\frac{1}{2}} \right), \left(x^{m-\frac{3}{2}}, v_x^{m-\frac{3}{2}} \right) \text{ and } \left(x^{m-\frac{5}{2}}, v_x^{m-\frac{5}{2}} \right) \right]$, the ion velocity near the left-hand boundary using the parabolic extrapolation scheme can be approximated as

$$v(x) = v_x^{m-\frac{5}{2}} + a \left(x - x^{m-\frac{5}{2}} \right) + b \left(x - x^{m-\frac{5}{2}} \right)^2, \quad (5.23)$$

where ‘ a ’ and ‘ b ’ are constants. The value of the constants are calculated. At the points $x = x^{m-\frac{1}{2}}$, the velocity is approximated as

$$v_x^{m-\frac{1}{2}} = v_x^{m-\frac{5}{2}} + a \left(x^{m-\frac{1}{2}} - x^{m-\frac{5}{2}} \right) + b \left(x^{m-\frac{1}{2}} - x^{m-\frac{5}{2}} \right)^2. \quad (5.24)$$

Solving above equation, we get

$$a = \frac{v_x^{m-\frac{1}{2}} - v_x^{m-\frac{5}{2}} - b \left(x^{m-\frac{1}{2}} - x^{m-\frac{5}{2}} \right)^2}{\left(x^{m-\frac{1}{2}} - x^{m-\frac{5}{2}} \right)}. \quad (5.25)$$

At the point $x = x^{m-\frac{3}{2}}$ the velocity is approximated as

$$v_x^{m-\frac{3}{2}} = v_x^{m-\frac{5}{2}} + a \left(x^{m-\frac{3}{2}} - x^{m-\frac{5}{2}} \right) + b \left(x^{m-\frac{3}{2}} - x^{m-\frac{5}{2}} \right)^2. \quad (5.26)$$

Using the value ‘ a ’ from Eq. (5.25) in Eq. (5.26), we obtain

$$v_x^{m-\frac{3}{2}} = v_x^{m-\frac{5}{2}} + \left[\frac{v_x^{m-\frac{1}{2}} - v_x^{m-\frac{5}{2}} - b \left(x^{m-\frac{1}{2}} - x^{m-\frac{5}{2}} \right)^2}{\left(x^{m-\frac{1}{2}} - x^{m-\frac{5}{2}} \right)} \right] \left(x^{m-\frac{3}{2}} - x^{m-\frac{5}{2}} \right) + b \left(x^{m-\frac{3}{2}} - x^{m-\frac{5}{2}} \right)^2. \quad (5.27)$$

Then from above equation, we obtain the value of ‘ b ’ as

$$b = \frac{\left(x^{m-\frac{5}{2}} - x^{m-\frac{3}{2}} \right) \left(v_x^{m-\frac{1}{2}} - v_x^{m-\frac{5}{2}} \right) - \left(x^{m-\frac{5}{2}} - x^{m-\frac{1}{2}} \right) \left(v_x^{m-\frac{3}{2}} - v_x^{m-\frac{5}{2}} \right)}{\left(x^{m-\frac{5}{2}} - x^{m-\frac{1}{2}} \right) \left(x^{m-\frac{5}{2}} - x^{m-\frac{3}{2}} \right) \left(x^{m-\frac{3}{2}} - x^{m-\frac{1}{2}} \right)}. \quad (5.28)$$

Using this value of ‘ b ’ in Eq. (5.25), the value of ‘ a ’ is obtained as

$$a = \frac{\left(x^{m-\frac{5}{2}} - x^{m-\frac{3}{2}} \right)^2 \left(v_x^{m-\frac{1}{2}} - v_x^{m-\frac{5}{2}} \right) - \left(x^{m-\frac{5}{2}} - x^{m-\frac{1}{2}} \right)^2 \left(v_x^{m-\frac{3}{2}} - v_x^{m-\frac{5}{2}} \right)}{\left(x^{m-\frac{5}{2}} - x^{m-\frac{1}{2}} \right) \left(x^{m-\frac{5}{2}} - x^{m-\frac{3}{2}} \right) \left(x^{m-\frac{3}{2}} - x^{m-\frac{1}{2}} \right)}. \quad (5.29)$$

Then using the value of constants ‘ a ’ and ‘ b ’ from Eq. (5.28) and (5.29) onto the Eq. (5.23), the ion velocity at the left-hand boundary is calculated as

$$v_\tau^i(x) = v_x^{m-\frac{5}{2}} - ax^{m-\frac{5}{2}} + b \left(x^{m-\frac{5}{2}} \right)^2. \quad (5.30)$$

5.5 Ion velocity distribution function

When we trace the ion trajectories for all n_{tra} injection velocities $v_{\tau L}^i$, we can calculate the corresponding intersection velocities Eq. (5.22) and the related distribution functions at all grid points x_j . The injection velocity from where we start are usually uniformly spaced, but the corresponding ion velocities at the other grid points, $0 \leq x_j \leq L$, are non-uniformly spaced and usually do not coincide with the fixed grid velocities, v_k . For our model, it is not necessary to know the ion distribution function at these uniformly spaced grid velocities. We can calculate the ion distribution function at the fixed grid points (position and velocity) by linear interpolation of the values associated with the trajectory intersection points to the nearest desired grid points [16].

5.6 Ion density distribution

The ion density distribution $n^i(x)$ is obtained from Distribution Function Approach (DFA). In the DFA, the ion density $n^i(x_j)$ is obtained by integrating the ion velocity distribution function over velocity space. For the plasma model, we obtain the ion distribution function only at the intersection points $[x_j, v_{\tau}^i(x_j)]$ and can also be obtained at the fixed grid points $[x_j, v_k]$ where the distribution function is given. The ion density at x_j , where the distribution functions $f^i(x_j, v_{\tau j}^i)$ and the intersection velocities of all n_{tra} ion trajectories $v_{\tau j}^i$ are given, may be obtained by the following discretized form:

$$n^i(x_j) = \frac{1}{2} \sum_{\tau=1}^{n_{tra}-1} [f^i(x_j, v_{\tau j}^i) + f^i(x_j, v_{\tau+1,j}^i)] (v_{\tau+1,j}^i - v_{\tau j}^i) \quad (5.31)$$

$$n^i(L) = \frac{1}{2} \sum_{\tau=1}^{n_{tra}-1} [f^i(L, v_{\tau L}^i) + f^i(L, v_{\tau+1,L}^i)] (v_{\tau+1,L}^i - v_{\tau L}^i). \quad (5.32)$$

5.7 Solution of Poisson's equation

After the calculation of the electron and ion densities respectively from Eq. (5.14) and Eq. (5.32), the space charge density distribution can be obtained from

$$\rho(x_j) = \sum_s q^s n^s(x_j) \quad (5.33)$$

$$= e[n^i(x_j) - n^e(x_j)]. \quad (5.34)$$

By the knowledge of the space charge distribution $\rho(x_j)$ from Eq. (5.33), we can solve the Poisson's Eq. (3.29) numerically to obtain the related new potential distribution, $\phi(x_j)$.

Using Eq. (5.13), the discretized form of Poisson's equation is given by

$$\frac{\phi_{j+1} - 2\phi_j + \phi_{j-1}}{(\Delta x)^2} = -\frac{\rho_j}{\epsilon_o}. \quad (5.35)$$

Now we write this equation for all internal grid points in the simulation region ($j = 2, 3, \dots, n_x - 1$) which yields the following $n_x - 2$ equations involving the n_x unknowns, $\phi_1, \phi_2, \dots, \phi_{n_x}$:

$$\phi_1 - 2\phi_2 + \phi_3 = -\frac{(\Delta x)^2}{\epsilon_o} \rho_2 \quad (5.36)$$

$$\phi_2 - 2\phi_3 + \phi_4 = -\frac{(\Delta x)^2}{\epsilon_o} \rho_3 \quad (5.37)$$

.

$$\phi_{n_x-2} - 2\phi_{n_x-1} + \phi_{n_x} = -\frac{(\Delta x)^2}{\epsilon_o} \rho_{n_x-1}. \quad (5.38)$$

We have fixed the potential values at the two boundaries as

$$\begin{aligned} \phi(x = L) &= \phi_{n_x} \\ &= \phi_L \end{aligned} \quad (5.39)$$

and

$$\begin{aligned} \phi(x = 0) &= \phi_1 \\ &= \phi_0. \end{aligned} \quad (5.40)$$

By solving the Eq. (5.36), Eq. (5.39) and Eq. (5.40) we now obtain the potential distribution, i.e. the potential values $\phi_1, \phi_2, \dots, \phi_{n_x}$ which can be expressed as a single matrix equation as

$$\begin{pmatrix} 1 & 0 & 0 & 0 & \dots & 0 \\ 1 & -2 & 1 & 0 & \dots & 0 \\ 0 & 1 & -2 & \dots & \dots & 0 \\ \dots & \dots & \dots & \dots & \dots & \dots \\ \dots & \dots & \dots & \dots & \dots & \dots \\ \dots & \dots & \dots & 1 & -2 & 1 \\ \dots & \dots & \dots & 0 & 0 & 1 \end{pmatrix} \begin{pmatrix} \phi_1 \\ \phi_2 \\ \vdots \\ \phi_{n_x-1} \\ \phi_{n_x} \end{pmatrix} = \begin{pmatrix} \phi_o \\ -\frac{(\Delta x)^2}{\epsilon_o} \rho_2 \\ \vdots \\ \vdots \\ -\frac{(\Delta x)^2}{\epsilon_o} \rho_{n_x} \\ \phi_L \end{pmatrix}. \quad (5.41)$$

The matrix on the left-hand side and the one at the right-hand side are known. In order to solve the matrix equation inverse of the first matrix is multiplied with the right-hand side matrix which is done using a simple command in MATLAB program.

5.8 Relaxation scheme

The exact solution of Poisson's equation converges only for short systems (a few Debye lengths). As the system length increases, small fluctuation of the potential causes unphysical accumulation of the charges and the scheme breaks down. To overcome this difficulty we use the relaxation scheme [21]. The numerically exact new potential distribution $\phi_{ex}^{(m)}(x_j)$ is obtained by numerically solving Eq. (5.41) which is linearly combined with the old potential distribution $\phi^{(m-1)}(x_j)$ to obtain the “re-adjusted” new potential distribution $\phi^{(m)}(x_j)$, which is actually used as the relevant result of the m^{th} iteration:

$$\phi^{(m)}(x_j) = w\phi_{ex}^{(m)}(x_j) + (1 - w)\phi^{(m-1)}(x_j), \quad (5.42)$$

where w is relaxation parameter, having with $0 < w < 2$.

5.9 Electric field calculation

Here, we will discuss how the electric field is calculated at all the grid points from a given potential profile, and how the field is calculated for the points lying between two grid points.

(a) Electric field at the inner grid points:

At the inner grid points $j = 1, 2, \dots, n_x - 1$, the electric field is obtained as

$$E(x) = -\frac{\phi(x_{j+1}) - \phi(x_{j-1})}{2\Delta x} \quad (5.43)$$

(b) Electric field at the left-hand boundary:

Near the left-hand boundary ($x = 0$) we assume, for the potential, the parabolic approximation as

$$\phi(x) = \phi_1 + ax + bx^2, \quad (5.44)$$

where $\phi_1 = \phi_0$ is the potential at $x = 0$.

For the second and third grid points, we have the two equations

$$\phi_2 = \phi_1 + a\Delta x + b(\Delta x)^2 \quad (5.45)$$

and

$$\phi_3 = \phi_1 + 2a\Delta x + 4b(\Delta x)^2 \quad (5.46)$$

respectively, from which the constants ‘ a ’ and ‘ b ’ can be obtained as

$$a = -\frac{3\phi_1 - 4\phi_2 + \phi_3}{2\Delta x} \quad (5.47)$$

and

$$b = -\frac{\phi_1 - 2\phi_2 + \phi_3}{2(\Delta x)^2}. \quad (5.48)$$

The electric field near $x = 0$ is obtained by taking the derivative of Eq. (5.44) as

$$E(x) = -\frac{d\phi(x)}{dx} \quad (5.49)$$

$$= -a - 2bx. \quad (5.50)$$

So that the electric field at the left-hand boundary is given by

$$E(x = 0) = -a \quad (5.51)$$

$$= \frac{3\phi_1 - 4\phi_2 + \phi_3}{2\Delta x}. \quad (5.52)$$

(c) Electric field at the right-hand boundary:

Near the right-hand boundary ($x = L$), we assume for the potential the parabolic approximation as

$$\phi(x) = \phi_{n_x-2} + c(x - x_{n_x-2}) + d(x - x_{n_x-2})^2, \quad (5.53)$$

where ϕ_{n_x-2} is the potential at the grid point $x_{n_x-2} \equiv L - 2\Delta x$. For the grid points x_{n_x-1} and x_{n_x} , we have the equations

$$\phi_{n_x-1} = \phi_{n_x-2} + c\Delta x + d(\Delta x)^2 \quad (5.54)$$

and

$$\phi_{n_x} = \phi_{n_x-2} + 2c\Delta x + 4d(\Delta x)^2 \quad (5.55)$$

respectively, from which the constants ‘ c ’ and ‘ d ’ can be obtained as

$$c = -\frac{\phi_{n_x} - 4\phi_{n_x-1} + 3\phi_{n_x-2}}{2\Delta x} \quad (5.56)$$

and

$$d = \frac{\phi_{n_x} - 2\phi_{n_x-1} + \phi_{n_x-2}}{2(\Delta x)^2}. \quad (5.57)$$

The electric field near $x = L$ is obtained by taking the derivative of Eq. (5.53) as

$$E(x) = -\frac{d\phi(x)}{dx} \quad (5.58)$$

$$= -c - 2d(x - x_{n_x-2}),$$

so that the electric field at the right-hand boundary is given by

$$\begin{aligned} E(x = L) &= -c - 4d\Delta x \\ &= -\frac{3\phi_{n_x} - 4\phi_{n_x-1} + \phi_{n_x-2}}{2\Delta x}. \end{aligned} \quad (5.59)$$

(d) The electric field at any point in the simulation region:

Once we have calculated the electric field at every grid point, the electric field at any point in the simulation region is obtained by linear interpolation between two nearest grid points x_j and x_{j+1} as

$$E(x) = \frac{(x_{j+1} - x)E_j + (x - x_j)E_{j+1}}{\Delta x}. \quad (5.60)$$

5.10 Iteration scheme

We are dealing with collisional, time independent system only. The initial-guess potential $\phi^{(0)}(x_j)$ is taken as input to the main Iteration Block (located between the points P and Q in Fig. (5.2), which will yield the first Iteration to the potential distribution $\phi^{(1)}(x_j)$. With the new potential as input, the main Iteration Block will be invoked again yielding $\phi^{(2)}(x_j)$ until the potential distribution has converged in the sense outlined in Sec. (5.11) below.

(a) Boundary conditions:

The boundary potentials $\phi(x = 0)$ and $\phi(x = L)$ and the boundary injection distribution functions $f^s(L, v)$ are to be provided as input parameters. Hence, they must be specified before entering the iteration scheme and are kept constant throughout the entire simulation.

(b) Initial guess to $\phi(x)$:

To start the scheme, we must suitably prescribe an initial-guess potential distribution. As we restrict ourselves to potential distributions $\phi(x)$, which decrease monotonically from $\phi(L) = 0$

to $\phi(0) = \phi_o < 0$. The starting potential distribution is chosen to be a linear interpolation between the potential values at the boundaries.

5.11 Main iteration block

Here we describe the main iteration scheme discussed in the Fig. (5.2). The main iteration block carries out the m^{th} iteration [i.e. it calculates the new distributions $\phi^m(x_j)$] for a given input (old) potential distribution $\phi^{m-1}(x_j)$ by performing the following three steps:

Step 1: The new electron density distribution $n^{e(m)}(x_j)$ is calculated analytically using Eq. (5.14). The new ion density $n^{i(m)}(x_j)$ is calculated by the distribution function approach(DFA). In DFA, the new ion densities are obtained by velocity-space integration of the new velocity distribution functions [cf. sec. 4.6 (a)].

Step 2: From the new densities $n^{s(m)}(x_j)$, obtained in step 1, the new space-charge density $\rho^{(m)}(x_j)$ is calculated using the Eq. (5.33).

Step 3: The new potential distribution $\phi^{(m)}(x_j)$ is calculated by solving the matrix Eq. (5.41) numerically, with the new space-charge density $\rho^{(m)}(x_j)$ inserted on the right-hand side.

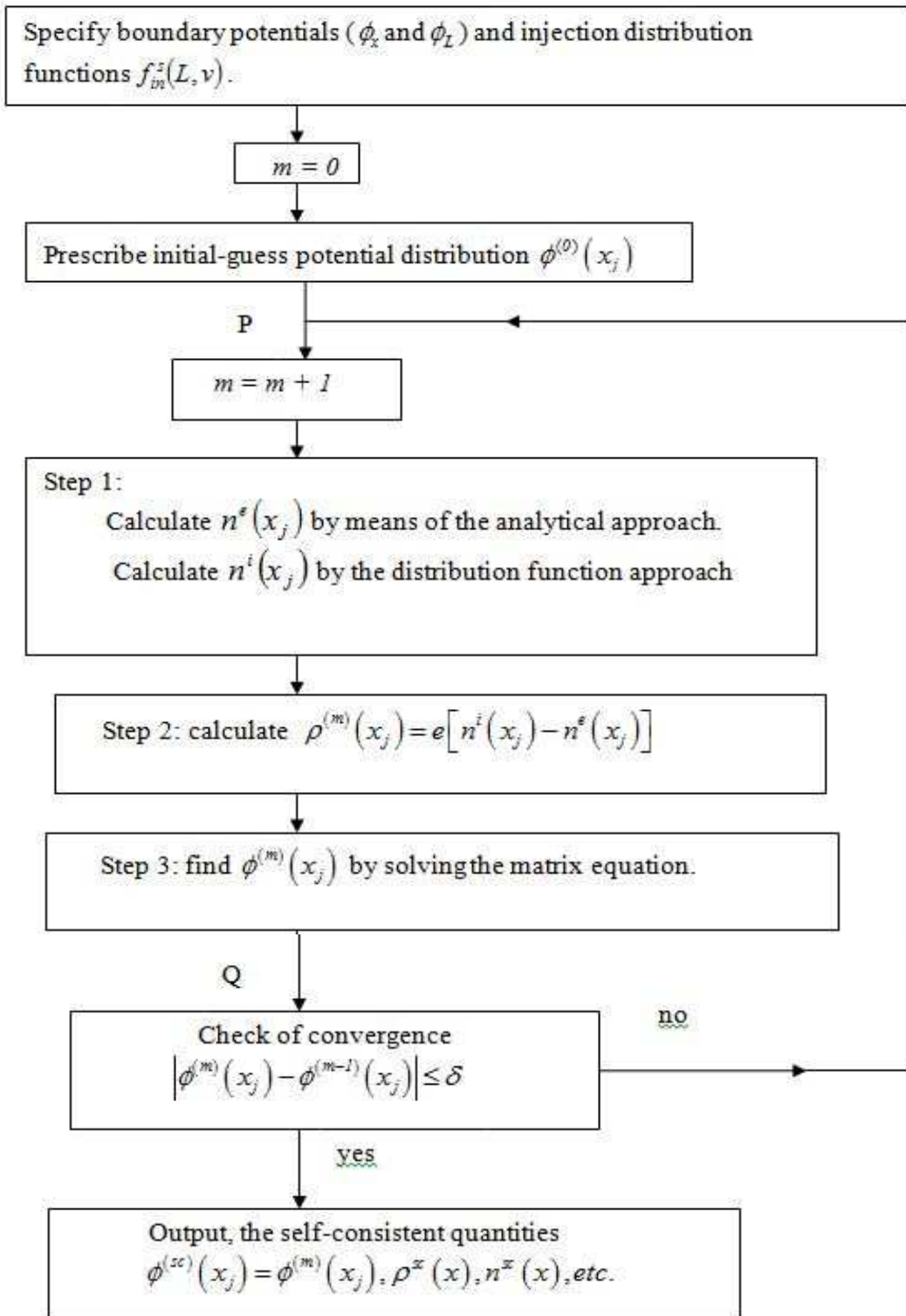


Figure 5.2: The iteration scheme.

5.12 Convergence check

The new potential distribution, $\phi^{(m)}(x_j)$, obtained in Step 3 of the main iteration block is compared with the old potential distribution, $\phi^{(m-1)}(x_j)$, and we consider the convergence to be reached if at each point x_j the condition

$$|\phi^m(x_j) - \phi^{(m-1)}(x_j)| \leq \delta \quad (5.61)$$

is satisfied, where δ is defined as accuracy parameter.

5.13 Numerical parameters

The Kinetic Trajectory Simulation is applied to our problem. We specifically consider the following parameters as given at the presheath side of the sheath-presheath boundary:

- Hydrogen plasma with plasma density $(n_{ps}) = 10^{18} \text{ m}^{-3}$.
- Electron temperature $(T_{ps}^e) = 10eV$, i.e. $10 \times 11604.9 \text{ K}$.
- Ion temperature $(T_{ps}^i) = 0.1T_{ps}^e eV$.
- Ion polytropic constant $(\gamma^i) = 3$.

The resulting dimensional sheath parameters at the sheath side of the sheath-presheath boundary are then obtained from the coupling scheme. We choose the sheath to be of width $10 \lambda_D^e$, where λ_D^e is the electron Debye length at the sheath entrance associated with the injected electrons.

The discrete ion injection velocities at the sheath entrance is discretized uniformly with 300 injection-velocity grid point such that the ion injection velocity grid step is considerably less than the ion thermal velocity. The region between $x = 0$ to L is discretized uniformly with 31 grid points. We define the system to have reached convergence (cf. sec. 5.12) if the maximum difference in potential values before and after iteration equals 10^{-5} V or less.

Chapter 6

Results and Discussion

In this section, the results obtained by simulation of 1d1v plasma sheath by introducing collision term which is characterized by α [cf. Section 4.1], are presented and discussed. The value of α represents the degree of collision, i.e. how frequent the collision occur. Lets take $\alpha = 0.01$ which implies that if a particle encounters 100 other particles it undergoes a single collision, $\alpha = 1$ corresponds to the case where every encounter is collision . For collisionless case $\alpha = 0$ and $0 < \alpha \leq 1$ for collisional case. The plasma sheath structure have been studied for different values of α , for the same presheath parameters. The final self consistent profile for ion and electron densities, total charge density, potential distribution, average velocity, and effective temperature within the sheath region have been plotted and discussed.

6.1 Ion density profile

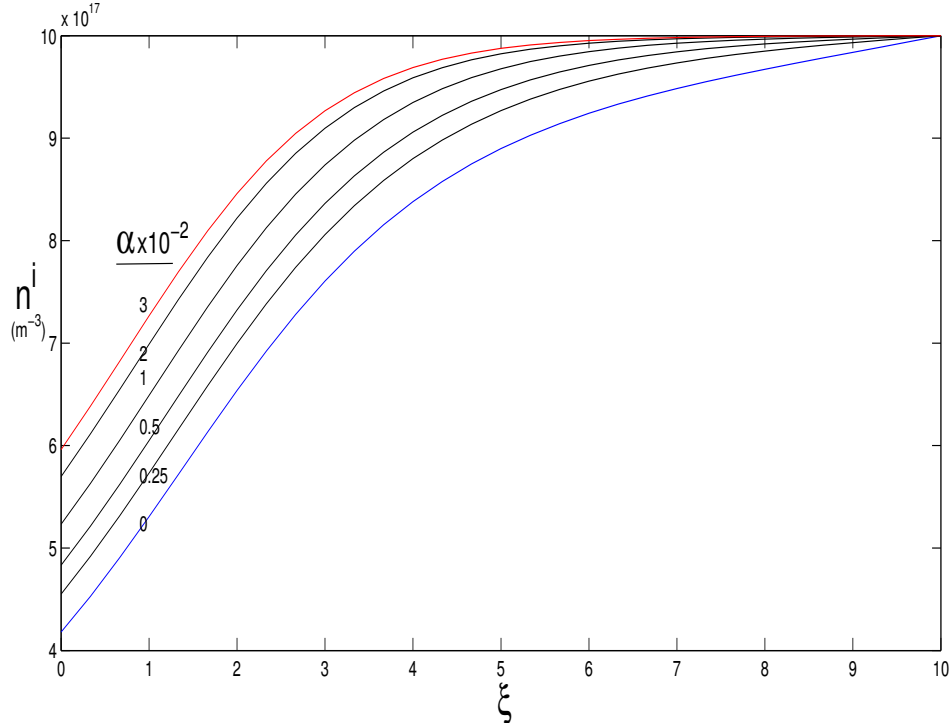


Figure 6.1: Self consistent ion density versus normalized distance for different values of α

The Fig. 6.1 shows the self consistent ion density versus normalized distance for different

values of α (degree of collision). In this chapter in all plots the distance from the wall is normalized with respect to electron Debye length at the sheath entrance and is termed normalized distance ($\xi = x/\lambda_D$). It is observed that the ion density decreases monotonically from the sheath entrance towards the wall acquiring its minimum value. The decrease in ion density is due to electrons have higher thermal velocities, reach the wall faster and hence the wall will be at negative potential. This repels further electrons thereby lowering their densities in the sheath region. This in turn causes the ion density to decrease conserving the flux. The plot for $\alpha = 0$, is shown to compare our result to previous work in collisionless cases. At sheath entrance the ion density is maximum and minimum at wall. As the degree of collision increases the rate by which ion density changes is different, starting with the same value of presheath ion density. At any given point in the sheath region the ion density is larger for higher value of α , the ion density is minimum for collisionless case, i.e., $\alpha = 0$, increases as we increase the value of α which explained on the fact that collision reduces the velocity of ion for flux conservation it's density must increases.

Increasing the value of α the rate at which the ion density increase is decreased and after certain value of α the ion density becomes saturated. Increasing the value of α from 0.2 to 0.3 the rate of increase of ion density is not sharp as compare α increases from 0 to 0.005. As we move towards the wall the ion density started decreasing at distance approximately $10\lambda_D$ from wall for $\alpha = 0$ (collisionless case), between $10\lambda_D$ and $9\lambda_D$ for $\alpha = 0.0025$, between $9\lambda_D$ and $8\lambda_D$ for $\alpha = 0.01$, between $8\lambda_D$ and $7\lambda_D$ for $\alpha = 0.02$, between $7\lambda_D$ and $6\lambda_D$ for $\alpha = 0.03$. Increasing the value of α the point after which the ion density starts to decrease rapidly shift towards the wall. The similar ion density profiles can be obtained for higher value of α but the profiles doesn't changes significantly.

6.2 Electron density profile

The Fig. 6.2 shows the self consistent electron density versus normalized distance for different values of α . The electron density decreases monotonically from sheath entrance to wall. Since

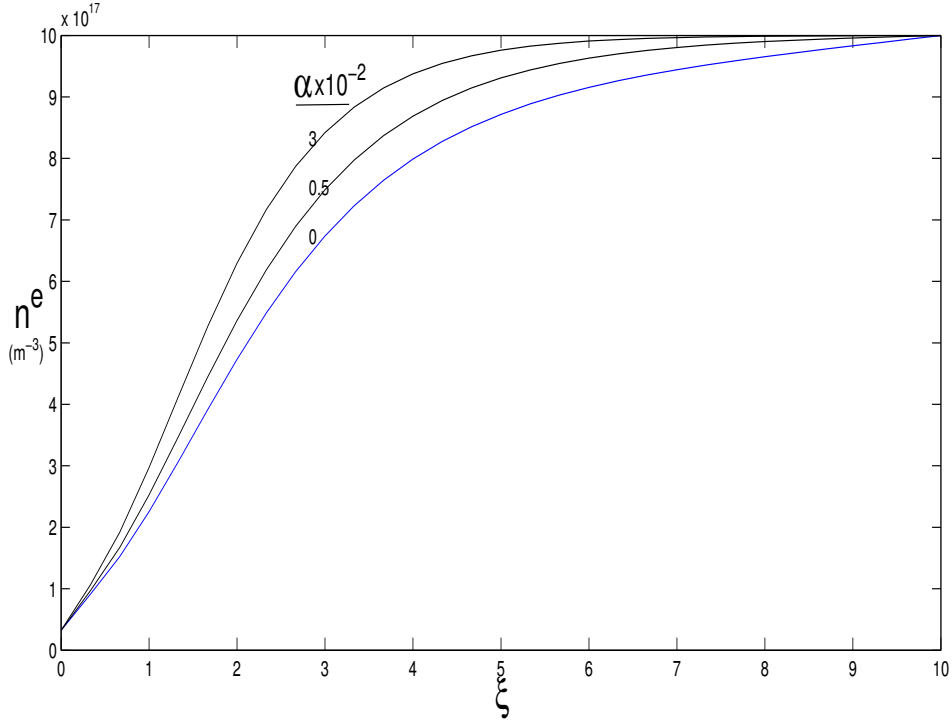


Figure 6.2: Self consistent electron density versus normalized distance for different values of α

electron density obtained analytically which explicit dependent on potential, as we fixed the wall potential constant causes the electron density constant what ever be the value of α . As we increase the value of α the electron density increases at any point in sheath region for flux conservation due to increase of ion density. At sheath entrance the electron density is maximum and minimum at wall. As the degree of collision increases the rate by which electron density changes is different, starting with the same value of presheath electron density. As increasing the value of α the rate at which the electron density increase is decreased and after certain value of α the electron density becomes saturated. Increasing the value of α from 0.005 to 0.3 the rate of increase of electron density is not sharp as compare α increases from 0 to 0.005, the electron density increases sharply. Increasing the value of α the point after which the electron density starts to decrease rapidly shift towards the wall. The similar electron density profiles can be obtained for higher value of α but the profiles doesn't changes significantly.

6.3 Comparison between ion and electron density profile

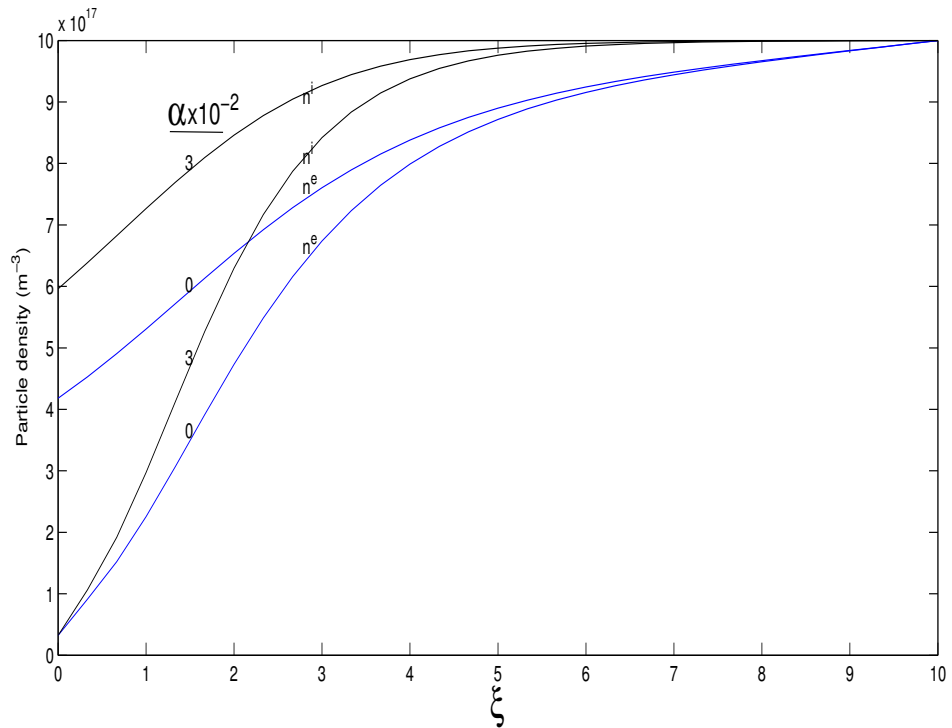


Figure 6.3: Self consistent ion and electron density versus normalized distance from the wall for different value of α

The Fig. 6.3 shows self consistent ion and electron density profiles both for collisionless ($\alpha = 0$) and typical collisional ($\alpha = 0.3$) case. In both case ion density is greater than electron density in sheath region and at wall but equal at sheath entrance (to satisfy quasineutrality condition). The electron density decreases more rapidly than ion density. Due to the negative potential of the wall, the electrons are reflected and hence the density of electrons as well as that of ions density decreases to conserve flux also the ion thermal velocity is less than that of electrons, the ion density exceeds the electron density so that the flux is conserved. For better comparison we can compare the density profile for different value of α as plotted in Fig. 6.1 and Fig. 6.2. instead of taking typical value of α .

6.4 Potential profile

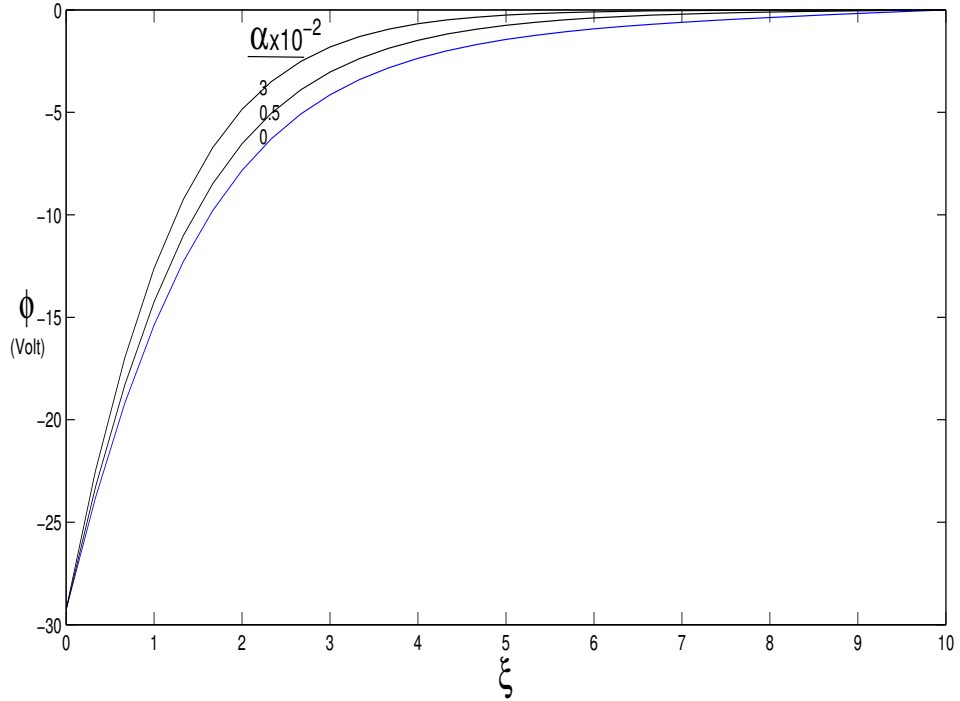


Figure 6.4: Self consistent potential versus normalized distance from the wall for different value of α

The Fig. 6.4 shows self consistent potential profile for both collisionless ($\alpha = 0$) and typical collisional ($\alpha = 0.03$) case. In both case negative potential increases monotonically from sheath entrance to wall. As we fixed the potential at wall and at sheath entrance fixed in simulation, the potential does not change at wall and sheath entrance but in other sheath region the potential has high value for high value of α . Also increasing the value of α the negative potential starts to increase at the point nearer to the wall. The similar potential profiles can be obtained for higher value of α but the profiles doesn't changes significantly. For more exact potential profile it is better to plot graph for different value of α .

6.5 Electric field profile

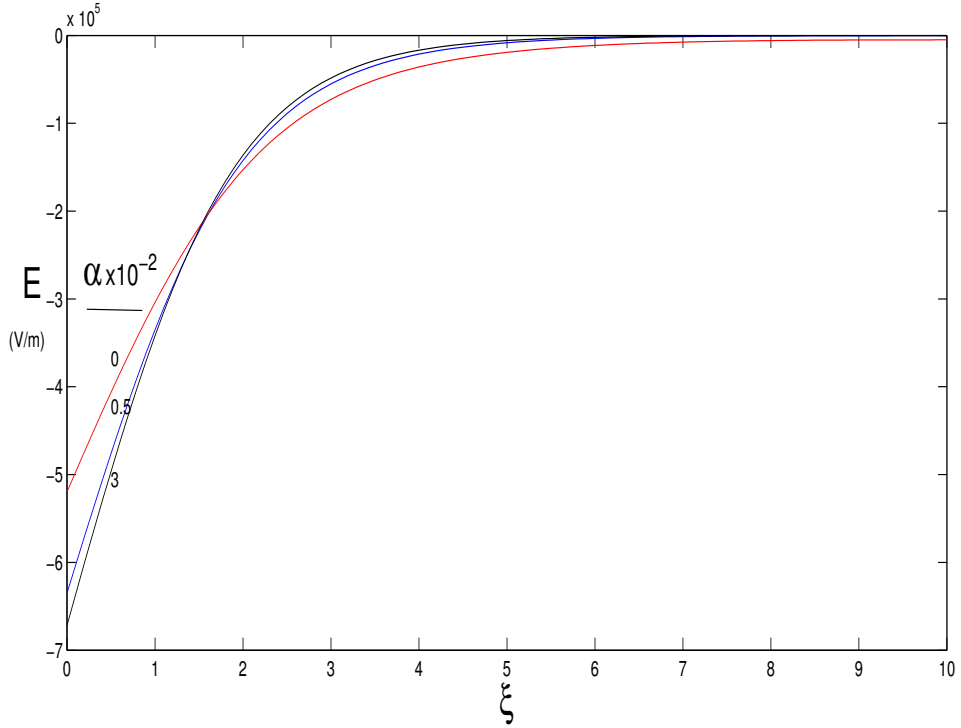


Figure 6.5: Self consistent electric field versus normalized distance from the wall for different value of α

The Fig. 6.5 shows the self consistent electric field profile versus the normalized distance from the wall for both collisionless ($\alpha = 0$) and collisional ($\alpha = 0.03, 0.005$) case. The electric field is always negative in the sheath region due to the negative potential and its magnitude increases towards the wall. Electric field is maximum at wall and minimum at sheath entrance. The field at wall is higher for higher value of α and becomes saturated as we increase the value of α due to high ion density but same electron density. Increasing the value of α from 0.005 to 0.3 the rate of increase of electric field is not sharp as compare α increases from 0 to 0.005, the electric field increases sharply. Increasing the value of α the point after which the electric field starts to increase rapidly shift towards the wall. The similar electric field profiles can be obtained for higher value of α but the profiles doesn't changes significantly.

6.6 Total charge density profile

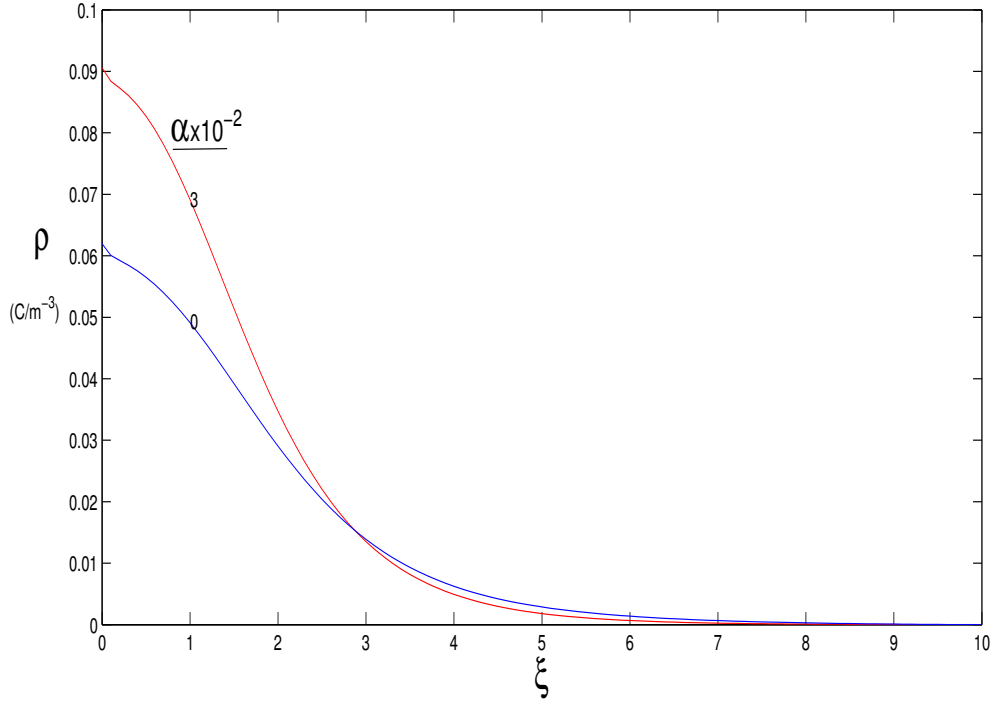


Figure 6.6: Self consistent total charge density versus normalized distance from the wall for different value of α

The Fig. 6.6 shows the typical self consistent charge density distribution versus the normalized distance from the wall for different value of α . The total charge density is zero at the sheath entrance (quasineutrality) and increases as we move towards the wall, where it acquires it's maximum. As the value of α increases the charge density at wall increases due to increase of electron and ion density. Increasing the value of α the point from which charge density rapidly start to increase shift to the wall. The similar charge density profiles can be obtained for higher value of α but the profiles doesn't changes significantly.

6.7 Average ion velocity profile

The Fig. 6.7 shows the self consistent average ion velocity versus the normalized distance from the wall for different value of α . The velocity of ion increases as we move from sheath entrance to wall in both collisional and collisionless cases. As the value of α increases the velocity of ion decreases due to collisional effect. The collision always decrease the velocity of colliding particle that same happen in the sheath region. The similar velocity profiles can be obtained for higher value of α but the profiles doesn't changes significantly.

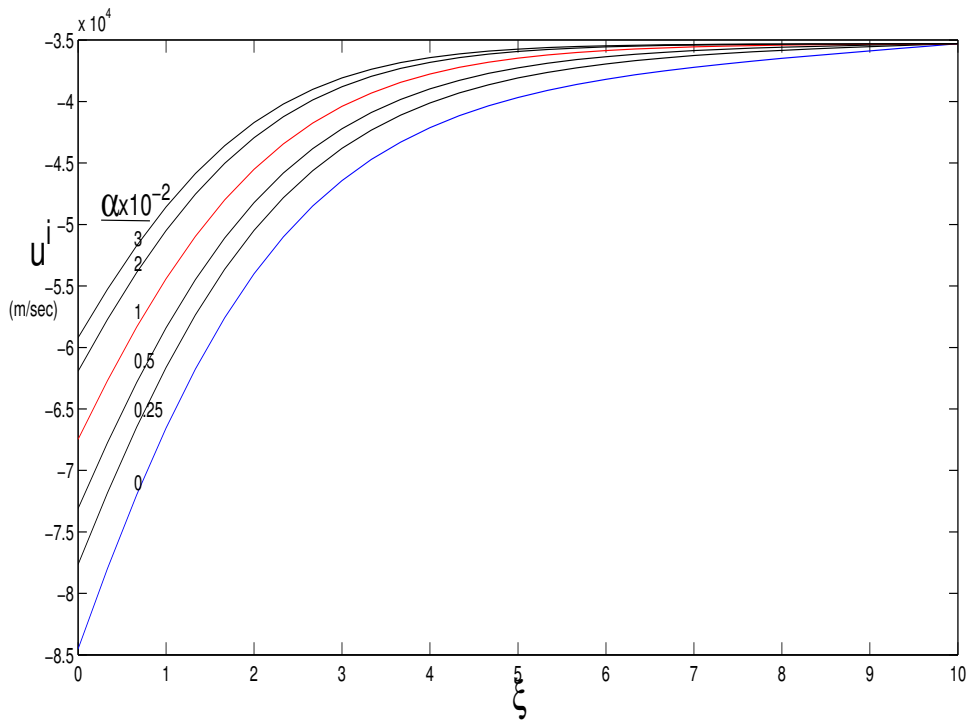


Figure 6.7: Self consistent ion average velocity versus normalized distance from the wall for different value of α

6.8 Ion effective temperature profile

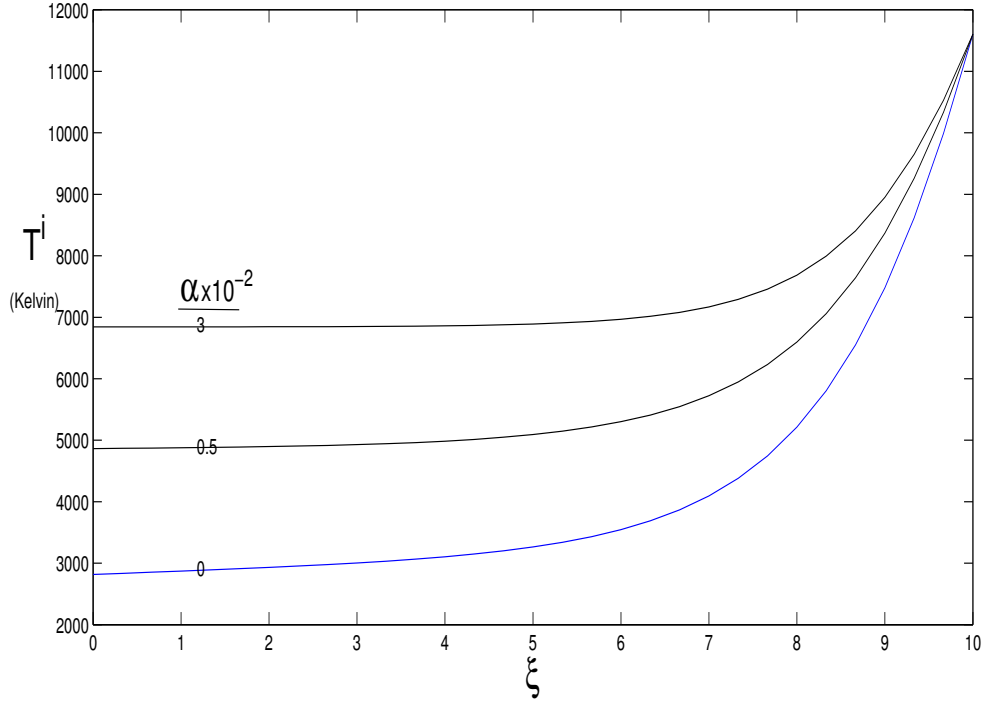


Figure 6.8: Self consistent ion effective temperature versus normalized distance from the wall for different value of α

The Fig. Fig. 6.8 shows the self consistent ion effective temperature profile versus normalized distance. The effective temperature decreases from sheath entrance to wall which is due to decrease in ion density towards the wall. As collision increases the effective temperature at any point in sheath region also increased due to increase in ion density by collisional effect. The similar temperature profiles can be obtained for higher value of α but the profiles doesn't changes significantly.

6.9 Discussion and conclusion

We have used a 1d1v kinetic model for the study of plasma sheath structure for different values of α (degree of collision) keeping other parameters the same. In all cases, the physical parameters such as potential, ion density, electron density, total charge density etc have very weak gradient close to the sheath entrance, however, they all have sharp gradient close to the wall.

The ion and electron density increases at any point in sheath as the value of α is increased. The ions are then accelerated towards the wall and are absorbed by the wall, decreasing the negative wall potential. This causes the increase in the electron density. However the system balances itself for higher n_i than n_e to conserve the flux (electron have higher mobility than ion) for all valid values of α .

Both the ion and electron density decrease gradually from the sheath entrance towards the wall. Precisely, the density of electron decreases faster than that of ion. This is due to the reflection of electrons by negative potential at the wall. The decrease in ion and electron density is less prominent as we increase the value of α at the sheath.

All sheath parameter measured above have great effect of α . If we compare the effect of α when its value close to 0 and for higher value, it is observed that when value of α are varied in lower region close to 0 effect the sheath structure highly than varying the value of α in higher region. From our simulation result we can say after certain value of α , the collision does not significantly effects the sheath structure.

The collision effect decrease the sheath width which can be explained by potential profile. The sheath entrance starts from where negative potential starts increase. As degree of collision increases the negative potential starts increase at the point nearer to the wall. This also explained by the total charge density. The plasma region is quasineutral region but sheath region is not quasineutral. From which the quasineutrality breaks we can say the sheath started.

The results discussed above suggest that sheath structure is greatly influenced by collision

at the sheath region. The work developed here starts a suitable basis for an important study in future, the main purpose being to arrive at more realistic collision models. Besides, our work is expected to provide necessary idea for the implantation of ions at material walls as well as in various applications of plasma.

The following cases may be considered in future work:

- (a) Time dependent cases
- (b) Magnetic field into consideration
- (c) Higher dimensional analysis
- (d) Considering the specific collision
- (e) Considering time dependent collision term
- (f) Kinetic treatment to electron

Appendix A

Matlab Files

In this section we present the MATLAB files.

(a) input file

```
alpha= input('Type the value of alpha') ;
```

```
% Basic parameters:
```

```
 $kB = 1.38062e - 23$ ; % Boltzmann constant
```

```
 $\epsilon_0 = 8.85419e - 12$ ; % permittivity of the medium
```

```
 $e = 1.602192e - 19$ ; % electronic charge
```

```
 $Ze = e$ ; % ion charge
```

```
 $M_i = 1.672e - 27$ ; % ion mass
```

```
 $M_e = 9.109e - 31$ ; % electron mass
```

```
 $\mu_e = M_e/M_i$ ; % electron to ion mass ratio
```

```
 $\gamma_{\text{ion}} = 3$ ; polytropic constant for ions(isothermal case)
```

```
% presheath parameters:
```

$Tpse = 10 * 11604.873;$ % electron temperature at presheath side

$Tpsi = 0.1 * Tpse;$ % ion temperature at presheath side

$nps = 1e18;$ % plasma density at presheath side

$cpsi = sqrt(k_B * (Tpse + gammai * Tpsi) / Mi);$ % ion acoustic velocity at presheath side

$upsi = -cpsi;$

% Normalized quantities:

$TpsiN = Tpsi / Tpse;$ % normalized ion temperature at preseath side

$upsiN = upsi / sqrt(2 * k_B * Tpse / Mi);$ % normalized ion acoustic velocity

% sheath parameters:

$JpsN = 0;$ %Normalized current density

$phiL = 0;$ % potential at $x = L$

$rhoL = 0;$ % charge density at $x = L$

$L = '10 * DLe';$ % system length

% numerical input parameters:

$ntra = 200;$

$phi0x = 'phi0 * (1 - X/L);$

$nx = 31;$ % number of x-grids

$dt = 1e - 11;$

$deltaphi = 1e - 5;$ % desired accuracy in the iteration

$w = .08;$ % signifies the relaxation parameters

$nv = 300;$ % number of velocity grid

$phifNi = linspace(-5, -0.001, 401);$ % initial guess (always negative)

$Tau_{min} = -5.8877254338;$ % lower limit of variable ‘Tau’. useless to keep below: -5.8877254338,
since $f \rightarrow 0.$

$TcLiNi = linspace(-5.88, 0, 90);$ % initial guess

$asymTcLiN = -4.5;$ % limit below which we use the asymptotic expression

(b) Distribution function for ions at injection

% specify the injection ion velocity distribution

function for specified velocity vx function $df = Dfun(v_x)$ global niL vmLi vtfi kB Tf Mi
vmaxLi vcLi

$df == niL * exp(-((vx - vmLi)/vtfi).^2) / sqrt(.5 * pi * kB * Tf / Mi) / (erf((-vmaxLi +$
 $vmLi)/vtfi) + erf((-vmLi + vcLi)/vtfi));$

(c) Poisson solver

% solves the poisson equation for given charge density and potential at the boundaries fixed
to some constant value

$MR(1) = phi(1); MR(nx) = phi(nx); MR(2 : nx - 1) = -dx^2 * rho(2 : nx - 1) / epsilon;$

$phin = MLMR'; phin = phin;$

$phin = w * phin + (1 - w) * phi; phin(1) = phi(1); phin(nx) = phi(nx);$

(d) Electric field calculation

Here we calculate the electric field to the given potential function

```
field = DFAEfield(x)
```

```
global Ef dx X nx
```

```
if x == 0
```

```
field = Ef(1);
```

```
elseif x == X(nx)
```

```
field = Ef(nx);
```

```
else
```

```
j = ceil(x/dx);
```

```
field = (Ef(j) * (X(j + 1) - x) + Ef(j + 1) * (x - X(j)))/dx;
```

```
end
```

(e) Coupling of the sheath with the presheath

```
% Coupling sheath with presheath.
```

```
% For given presheath plasma parameters (nps, Tpsi, Tpse, Jps, gammai, mu, etc.)
```

```
% this program
```

```
% calculates sheath plasma parameters (Ai, Ae, vcLi, vmLi, Tfe, Tfi, phi0, etc.)
```

```
% required for our 1d1v plasma-sheath simulation
```

```
% This proceeds as following:
```

```
% 1) Provide the name of your input file, where all required input parameters are
```

```
% specified.
```

```
% 2) Solves the electron irreducible equation to obtain 'phifN', and then the other
```

% corresponding

% electron parameters (TfeN, AeN, phi0N, etc.) are calculated.

% 3) Solves the ion irreducible equation to obtain 'TauLiN', and then the other

% corresponding

% ion parameters (TfiN, AiN, vmLiN, vcLiN, etc.) are calculated.

% 4) Once all normalized parameters are known, the dimensionless physical

% parameters are calculated

% using their respective normalizing equations.

% close all,

% clear all

% solving the electron irreducible equation for 'phifN' ---start --- :

% Calculating the lhs (Le) of the equation (independent of 'JpsN' and 'TpsiN'):

% Calculating other parameters:

for rphifN = 1 : length(phifNi)

phifN = phifNi(rphifN);

Ce = 1 + erf(sqrt(-phifN));

De = exp(phifN);

TfeN = 1/abs(1 - sqrt(-4 * phifN/pi) * De/Ce - 2/pi * (De/Ce)^2);

Le(rphifN) = De/Ce * sqrt(TfeN/pi);

% lhs of the electron irreducible equation

end % for r = 1 : length(phifNi)

% Calculating the rhs (Re) of the equation (function of 'JpsN', 'TpsiN', 'gammai' and 'mu'):

*Re = sqrt(mu) * (JpsN + sqrt(.5 * (1 + gammai * TpsiN))); % rhs of the equation*

phifN_sol = interp1(Le, phifNi, Re); % Interpolating for the solution (phifN) for which

Le = Re.

% Thus obtained 'phifN_sol' is the required value.

if isnan(phifN_sol)

disp('Could not find the solution. Change the input-range for phifN and start again.')

pause

else

phifN = phifN_sol

Ce = 1 + erf(sqrt(-phifN));

De = exp(phifN);

*TfeN = 1/abs(1 - sqrt(-4 * phifN/pi) * De/Ce - 2/pi * (De/Ce)^2);*

AeN = 1/Ce/sqrt(TfeN);

% solving the ion irreducible equation for 'phifN'---*end*---

% solving the ion irreducible equation for 'TcLiN'---*start*---

% Calculating the rhs (Ri) of the equation (function of 'phifN', independent of 'JpsN' and 'TpsiN'):

Ri = (sqrt(pi) + De/Ce/sqrt(-phifN))/TfeN; % Calculating the lhs (Li) of the equation:

$rr = 1;$ for $r = 1 : length(TcLiNi)$

$TcLiN = TcLiNi(r);$

if $TcLiN < asymTcLiN]$ % using asymptotic expansion: $erf(x) = 1 - exp(-x^2)/sqrt(pi)/x * (1 - 1/2/x^2 + 3/2^2/x^4 - 1.3.5/2^3/x^6 + \dots)$

$Ci = exp(-TcLiN^2)/abs(TcLiN)/sqrt(pi)*(1 - .5/TcLiN^2 + .75/TcLiN^4 - 15/8/TcLiN^6 + 105/16/TcLiN^8 - \dots 945/32/TcLiN^10) + 10395/64/TcLiN^12 - 135135/128/TcLiN^14 + 2027025/256/TcLiN^16 - 34459425/512/TcLiN^18 + \dots 654729075/1024/TcLiN^20 - 13749310575/2048/TcLiN^22 + 316234143225/4096/TcLiN^24 - 7905853580625/8192/TcLiN^26);$

else % if $TcLiN < asymTcLiN$

$Ci = 1 + erf(TcLiN);$ % if $TcLiN < asymTcLiN$

end

$Di = exp(-TcLiN^2);$

$TfiN = TpsiN/abs(1 - 2 * TcLiN * Di/Ci/sqrt(pi) - 2 * (Di/Ci)^2/pi);$

$vmLiN = -sqrt(0.5 * (1 + gammai * TpsiN)) + Di/Ci * sqrt(TfiN/pi);$

$a = vmLiN/sqrt(TfiN);$ % abbreviated for simplicity

if $TcLiN < -a$ % checking the integrability

% Integrating:

$Tau = linspace(Tau_min, TcLiN, ntra);$ % Discretizing for integration

$dTau = Tau(2) - Tau(1);$ % Width of the Tau-grid

for $rTau = 1 : ntra$

$FnTau(rTau) = exp(-Tau(rTau)^2)/(Tau(rTau) + a)^2;$

end

$LHS = dTau * (sum(FnTau) - 0.5 * (FnTau(1) + FnTau(ntra)));$

$Li(rr) = LHS/Ci/TfiN;$

$TcLiNM(rr) = TcLiN;$ % storing the values for which the equation is integrable.

$rr = rr + 1;$

end % if $TcLiN < -a$

end

for $r = 1 : length(phifNi)$

% obtaining the solution by locating the point of intersection of 'Li' and 'Ri':

%*plot(TcLiNM, Li)*

%*hold*

%*plot([min(TcLiNM) max(TcLiNM)],[Ri Ri],'k--')*

$TcLiN_{sol} = interp1(Li, TcLiNM, Ri);$ % required solution

% This method of obtaining the solution can be RISKY. The point where we have found ' $Li = Ri$ ' is

% the point of marginal validity of the Bohm criterion, which, in our case, is $Li \leq Ri$.

% When we consider the marginal point it may be possible that because of numerical limitations it

% lies in fact in the region, where the Bohm criterion is not satisfied. Hence, in order to

% be sure we take a point very close to the zero-point but still lying in the negative side of

```

% sure side of ( $Li - Ri$ ), so that we may say that  $Li \leq Ri$ , in place of  $Li \leq Ri$ .
%
% We have tested it many times and concluded that it has also negligible effect to the
%
% other ion parameters derived therefrom.  $a = find(Li - Ri < 0)$ ;
%
% points where  $Li < Ri$   $a = a(length(a))$ ;
%
% points where  $Li < Ri$ ,  $a = a(length(a))$ ;
%
% points closest to the zero-point but still  $Li < Ri$   $TcLiN\_sol = TcLiNM(a)$ ;
%
% value of the closest point to the zero-point  $\rightarrow Li \leq Ri$ 
%
% plot (TcLiNM(a), Li(a), 'mo') % solving the ion irreducible equation for 'TcLiN' --
% end --
%
% calculating other dimensionless ion parameters:
%
% Thus obtained 'TcLiN_sol' is the required value. if  $isnan(TcLiN\_sol)$ 
%
% disp('Could not find the solution. Change the input-range for TcLiN and start again.')
%
% pause
%
% else
%
%  $TcLiN = TcLiN\_sol$ 
%
% Calculating other parameters:
%
% if  $TcLiN < asymTcLiN$ 
%
% using asymptotic expansion:
%

$$erf(x) = 1 - exp(-x^2)/sqrt(pi)/x * (1 - 1/2/x^2 + 3/2^2/x^4 - 1.3.5/2^3/x^6 + \dots)$$


```

$$Ci = \exp(-TcLiN^2) / \text{abs}(TcLiN) / \sqrt{\pi} * (1 - .5/TcLiN^2 + .75/TcLiN^4 - 15/8/TcLiN^6 + 105/16/TcLiN^8 - \dots 945/32/TcLiN^{10}) + 10395/64/TcLiN^{12} - 135135/128/TcLiN^{14} + 2027025/256/TcLiN^{16} - 34459425/512/TcLiN^{18} + \dots 654729075/1024/TcLiN^{20} - 13749310575/2048 316234143225/4096/TcLiN^{24} - 7905853580625/8192/TcLiN^{26});$$

else % if $TcLiN < \text{asymTcLiN}$

$$Ci = 1 + \text{erf}(TcLiN);$$

end

% if $TcLiN < \text{asymTcLiN}$

$$Di = \exp(-TcLiN^2);$$

$$TfiN = TpsiN / \text{abs}(1 - 2 * TcLiN * Di / Ci / \sqrt{\pi}) - 2 * (Di / Ci)^2 / \pi;$$

$$vmLiN = -\sqrt{0.5 * (1 + \text{gammai} * TpsiN)} + Di / Ci * \sqrt{TfiN / \pi};$$

$$AiN = 1 / Ci / \sqrt{TfiN};$$

$$vcLiN = vmLiN + TcLiN * \sqrt{TfiN};$$

end % if $\text{isnan}(TcLiN_sol)$

end

% calculating dimensional physical parameters:

% electron dimensional parameters:

$$Tfe = TfeN * Tpse;$$

$$vtfe = \sqrt{2 * kB * Tfe / Me};$$

$$Ae = AeN * nps * \sqrt{2 * Me / \pi / kB / Tpse};$$

$$neL_- = Ae * vtfe * \sqrt{\pi} / 2;$$

$phi0 = phifN * kB * Tfe/e;$

$\%$ ion dimensional parameters:

$Tfi = TfiN * Tpse;$

$vtfi = sqrt(2 * kB * Tfi / Mi);$

$Ai = AiN * nps * sqrt(2 * Mi / pi * kB / Tpse);$

$niL = nps;$

$vmLi = vmLiN * sqrt(2 * kB * Tpse / Mi);$

$vcLi = vcLiN * sqrt(2 * kB * Tpse / Mi);$

(f) Ion density in DFA

$Q = Ze * dt / Mi;$ $\%$ defined for simplicity

$for T = 1 : ntra$ $\%$ selecting an ion trajectory

$m = 1;$ $\%$ initial time count

$VxL = VLi(T);$ $\%$ ion velocity for the selected trajectory at injection

$Vm(m) = vxL;$ $\%$ Starting velocity for ions at the injection(injection velocity)

$Xm2(m) = L + .5 * vxL * dt + Q * dt * DFAEfield(L) / 8;$ $\%$ moving by $dt/2$ for time centering(new starting position)

$if Xm2(1) <= X(nx - 1);$

$disp('Time step is too large. Press any key to continue.')$

pause

end

while $Xm2(m) > 0$ and $Xm2(m) \leq L$ % solving the equation of motion until the ion crosses

$x = 0$ or $x = L$ plane

$m = m + 1$; % next time step

$Vm(m) = Vm(m - 1) + Q * DFAEfield(Xm2(m - 1));$

$Xm2(m) = Xm2(m - 1) + dt * Vm(m);$

end

for $rr = 1 : m - 1$;

$Vm2(r) = 0.5 * (Vxm(r) + Vxm(r + 1));$

end

$Xt = [L, Xm2(1 : m - 1)]; Vt = [Vm2];$

$a = ((Xt(m - 2) - Xt(m))^2 * (Vt(m - 1) - Vt(m - 2)) - (Xt(m - 2) - Xt(m - 1))^2 * (Vt(m) - Vt(m - 2)))/(Xt(m - 2) - Xt(m - 1))/(Xt(m - 2) - Xt(m))/(Xt(m - 1) - Xt(m));$

$b = ((Xt(m - 2) - Xt(m)) * (Vt(m - 1) - Vt(m - 2)) - (Xt(m - 2) - Xt(m - 1)) * (Vt(m) - Vt(m - 2)))/(Xt(m - 2) - Xt(m - 1))/(Xt(m - 2) - Xt(m))/(Xt(m) - Xt(m - 1));$

$vx0 = Vt(m - 2) + a * Xt(m - 2) + b * Xt(m - 2)^2;$

$Xt = [Xt, 0]; Vt = [Vt, vx0];$ % Position (from x=L to x=0) and the corresponding velocities along the trajectory

$Vti = interp1(Xt, Vt, X);$ % Interpolating for the velocity at fixed grid(x)

$Vi(T, :) = Vti;$

$Is(T) = alpha * cps * L / (DLe)^2 * abs(VLi(T));$ % collision integral

$Df(T) = dfun(VLi(T)) + Is(T);$

```
clearVmVm2VtVtiXm2Xtabmrvx0
```

```
end
```

```
% ni calculating with interpolating onto the fixed velocity grid points
```

```
ni = zeros(1, nx);
```

```
for j = 1 : nx;
```

```
Vxi = Vi(:, j);
```

```
for T = 1 : ntra - 1
```

```
ni(j) = ni(j) + .5 * (Df(T) + Df(T + 1)) * abs(Vxi(T + 1) - Vxi(T));
```

```
end
```

```
clearVxiT
```

```
end
```

```
%% calculates average velocity for ions at any point X
```

```
ui = zeros(1, nx);
```

```
for j = 1 : nx;
```

```
Vxi = Vi(:, j);
```

```
for T = 1 : ntra - 1
```

```
j = 1 : nx;
```

```
ui(j) = ui(j) + 0.5 * (Df(T + 1) * Vxi(T + 1) + Df(T) * Vxi(T)) * abs(Vxi(T + 1) - Vxi(T)) / (ni(j) + .5);
```

```
end
```

```
clearVxiT
```

end

(g) Main command file for DFA

```
close all, clear all, global niL vmLi vtfi kB Tfi Mi vmaxLi vcLi Ef dx X nx alpha
% input('Type the name of your input file:');
```

Input;

CouplingPSandS; % gives input parameters for sheath simulation,

$uLe = -vtfi * De/Ce/sqrt(pi); uLi = vmLi - vtfi * Di/Ci/sqrt(pi);$

$DLe = sqrt(epsilon * kB * Tfe/neL/e^2);$

$L = eval(L);$

$vmaxLi = Tau_{min} * vtfi - vmLi;$

$I = 1;$ % Initializing the number of iteration counter

$X = linspace(0, L, nx);$

$dx = X(2) - X(1);$

$VLi = linspace(vmaxLi, vcLi, ntra);$

$dVLi = abs(VLi(2) - VLi(1));$

if $dx/DLe > .8$

disp(' Attention: Your grid width is comparable/larger than Debye length.')

dx , DLe

disp('Press ENTER to continue or CTRL-C to stop.')

pause

end

phi = eval(phi0x); *phi*(1) = phi0; *phi*(nx) = phiL; % load potential

for *j* = 2 : nx - 1

Ef(*j*) = .5 * (*phi*(*j* - 1) - *phi*(*j* + 1)) / *dx*;

end

Ef(1) = .5 * (3 * *phi*(1) - 4 * *phi*(2) + *phi*(3)) / *dx*;

Ef(nx) = .5 * (-3 * *phi*(nx) + 4 * *phi*(nx - 1) - *phi*(nx - 2)) / *dx*;

*DA*iondensity

ne = *neL* * exp(*e* * *phi* / *kB* / *Tfe*) * (1 + erf(sqrt(*e* * (*phi* - *phi*(1)) / *kB* / *Tfe*)));

ni = *niL* * *ni* / max(*ni*); *ne* = *niL* * *ne* / max(*ne*); *nin* = *ni* / *niL*; *ui* = *uiL* * *ui* / max(*ui*); *rho* = *Ze* * *ni* -

d = -2 * ones(1, nx); *d*(1) = 1; *d*(nx) = 1; *u* = ones(1, nx - 1);

ML = diag(*d*) + diag(*u*, 1) + diag(*u*, -1); *ML*(1, 2) = 0; *ML*(nx, nx - 1) = 0;

clear *d* *u*

*Poisson*solver; while max(abs(*phin* - *phi*)) > *deltaphi*

fluctuation = max(abs(*phin* - *phi*))

phi = *phin*;

for *j* = 2 : nx - 1

Ef(*j*) = .5 * (*phi*(*j* - 1) - *phi*(*j* + 1)) / *dx*;

end

```

 $Ef(1) = .5 * (3 * phi(1) - 4 * phi(2) + phi(3)) / dx;$ 
 $Ef(nx) = .5 * (-3 * phi(nx) + 4 * phi(nx - 1) - phi(nx - 2)) / dx;$ 
 $DAiondensity;$ 
 $ne = neL * exp(e * phi / kB / Tfe) * (1 + erf(sqrt(e * (phi - phi(1)) / kB / Tfe)));$ 
 $ni = niL * ni / max(ni); ne = niL * ne / max(ne);$ 
 $nin = ni / max(ni);$ 
 $nen = ne / max(ne);$ 
 $vcLe = sqrt(-2 * e * phi0 / Me);$ 
 $ui = uLi * ui / max(ui);$ 
 $rho = Ze * ni - e * ne;$ 
 $poissonsolver;$ 
 $end$ 
 $phi = phin;$ 
 $DAiondensity;$ 
 $ne = neL * exp(e * phi / kB / Tfe) * (1 + erf(sqrt(e * (phi - phi(1)) / kB / Tfe)));$ 
 $ni = niL * ni / max(ni); ne = niL * ne / max(ne); nin = ni / niL; nen = ne / max(ne);$ 
 $ui = uiL * ui / max(ui); uin = ui / max(ui);$ 
 $rho = Ze * ni - e * ne;$ 
 $x = X / DLe;$ 
 $Ef = Ef; Ef = Ef / max(Ef);$ 
 $plot(x, phin, 'r'), xlabel('normalised distance'), ylabel('phin')$ 

```

Bibliography

- [1] I. Langmuir, *Phys. Rev.* **33**, 954 (1929)
- [2] W. Crook, *Radiant matter*, (1878). University of Texas Press (2012)
- [3] J. A. Bittencourt, *Fundamentals of Plasma*
- [4] F. F. Chen, *Introduction to Plasma Physics and Controlled Nuclear Fusion, Plenum Press (1974) Physics*, Springer-Verlag (2004)
- [5] H. A. Bethe, C. L. Crichtchfield, *Phys. Rev.*
- [6] K. U. Riemann, *J. Phys. D. Appl. Phys.* **24**, 493 (1991)
- [7] K. U. Riemann, *J. Tech. Phys.* (Special Issue) **41**(1), 89 (2000) **54**, 248 (1938)
- [8] D. Bohm, *The Characteristic of Electrical Discharges in Magnetic Fields*, Edited by A. Guthry and R. K. Wakerling, McGraw-Hill (1949)
- [9] B. N. Chakraborty, *Principles of Plasma Physics*, New Age International Pvt. Ltd; New Delhi, **Chap. 6**, (2003)
- [10] T . E. Sheridan@ and J. Goree, *Collisional plasma sheath model*, (1991)
- [11] S.Farhad Masoudi, Shadi S. Esmaeili, Shima Jazavandi, *Ion dynamics in plasma sheath under the effect of EXB and collision force*, **Vacuum**,382-386 (2009)
- [12] S. Farhad Masoudi, *Effect of on plasma sheath in magnetic field*, **Vacuum**, 871-874 (2006)

- [13] H.-B. Valentinia, *Bohm criterion for the collisional sheath*, **Department of Physics, University of Greifswald, Greifswald, Germany**, (1996)
- [14] M. Goswami, H. Ramachandran, *Phys. Plasmas* **6**(12), 4522 (1999)
- [15] Rui Rosa, *Properties of the collisional plasma sheath with ionizations*, **J. Phys. A: Math., Nucl. Gen., Vol. 7**, no 4 (1994)
- [16] R. Khanal, *A Kinetic Trajectory Simulation Model for Bounded Plasmas*, PhD Thesis, University of Innsbruck, Austria (2003)
- [17] R N Franklin, *There is no such thing as a collisionally modified Bohm criterion*, **Institute of physics publishing**, 28212824 (2003)
- [18] V.Godyak, *phys. Plasma*, **11**(8),80 (1982)
- [19] M. A. Sobolewski, *J. Appl. Phys.* **95**, 4593 (2003)
- [20] P. M. Bellan, *Fundamental of Plasma Physics*, Cambridge University Press (2004)
- [21] W. H. Press, S. A. Teukolsky, W. T. Vetterling, B. P. Flannery, *Numerical Recipes*, Cambridge University Press (1989)
- [22] T. Nath Chetry, *Effect of Polytropic constant on particle Densities in Plasma Sheath* , M. Sc. Thesis, Tribhuvan University, Kathmandu, Nepal (2012)
(1982) R. Behrisch, Plenum Press (1986)